

1 **Transcriptome analysis provides genome annotation and expression profiles in the**
2 **central nervous system of *Lymnaea stagnalis* at different ages**

3

4 Martina Rosato^{1,3}, Brittany Hoelscher^{1,3}, Zhenguo Lin¹, Chidera Agwu¹, Fenglian Xu^{1,2,3*}

5 ¹ Department of Biology, College of Arts and Sciences, Saint Louis University, St. Louis,
6 MO, United States.

7 ² Department of Pharmacology and Physiology, Saint Louis University, School of Medicine, St.
8 Louis, MO, United States

9 ³ Henry and Amelia Nasrallah Center for Neuroscience, Saint Louis University, St. Louis,
10 MO, United States.

11

12 *Corresponding Author: Dr. Fenglian Xu

13 Email: fenglian.xu@slu.edu

14

15

16

17 Impact Statement (15-30 words)

18 This study provides the first transcriptome analysis and gene annotation of *Lymnaea*
19 *stagnalis* CNS from young, adult, and old animals, contributing to the largest and updated
20 *Lymnaea stagnalis* CNS transcriptomes.

21

22

23

24

25

26 **Abstract**

27 Molecular studies of the freshwater snail *Lymnaea stagnalis*, a unique model organism for
28 neurobiology research, has been severely hindered by the lack of sufficient genomic
29 information. As part of our ongoing effort studying *L. stagnalis* neuronal growth and
30 connectivity at various developmental stages, we provide the first age-specific transcriptome
31 analysis and gene annotation of young, adult, and old *L. stagnalis* central nervous system
32 (CNS). RNA sequencing using Illumina NovaSeq 6000 platform produced 56-69 millions of
33 150 bp paired-end reads, and 74% of these reads were mapped to the draft genome of *L.*
34 *stagnalis*. We provide gene annotations for 32,288 coding sequences with a minimum of 100
35 codons, contributing to the largest number of annotated genes for the *L. stagnalis* genome to
36 date. Lastly, transcriptomic analyses reveal age-specific differentially expressed genes and
37 enriched pathways in young, adult, and old CNS. These datasets represent the largest and
38 most updated *L. stagnalis* CNS transcriptomes.

39

40 **Introduction**

41 The freshwater snail *Lymnaea stagnalis* belongs to the phylum Mollusca, class Gastropoda
42 (Kuroda & Abe, 2020). Like its counterpart, the sea slug *Aplysia californica*, *L. stagnalis* has
43 served as an important mollusc model organism for the neurobiology field since the 1970s
44 due to its simple central nervous system (CNS) (Fodor, Hussein, Benjamin, Koene, & Pirger,
45 2020). *L. stagnalis* CNS contains a total of 20,000-25,000 neurons organized in a ring of 11
46 connected ganglia. The neurons are large in size (up to ~100 µm in diameter) and easily
47 recognizable, making them a perfect target for *in vitro* and *in vivo* studies. Many studies have
48 used this model to investigate the fundamental mechanisms of neuronal networks involved in
49 various behaviours including feeding (Kojima, Nanakamura, Nagayama, Fujito, & Ito, 1997;
50 Yeoman, Kemenes, Benjamin, & Elliott, 1994), respiration (Haque et al., 2006; Taylor &
51 Lukowiak, 2000), locomotion (Syed & Winlow, 1991; Vorontsov, Tsyganov, & Sakharov,
52 2004), and reproduction (Hermann, de Lange, Pieneman, ter Maat, & Jansen, 1997; Jimenez
53 et al., 2004). Studies have also focused on high cognitive behaviours, including learning and
54 memory (Dodd, Rothwell, & Lukowiak, 2018; Sunada et al., 2017; Swinton et al., 2019; Tan
55 & Lukowiak, 2018), as well as deciphering cellular mechanisms of synapse formation and
56 synaptic plasticity during development (Getz, Wijdenes, Riaz, & Syed, 2018; Mersman, Jolly,
57 Lin, & Xu, 2020; Onizuka et al., 2012). *L. stagnalis* has also recently gained increasing
58 popularity for the investigation of brain aging and neurodegenerative diseases such as
59 Parkinson's disease and Alzheimer's disease (Arundell et al., 2006; de Weerd, Hermann, &
60 Wildering, 2017; Ford, Crossley, Vadukul, Kemenes, & Serpell, 2017; Hermann, Perry,
61 Hamad, & Wildering, 2020; Maasz et al., 2017). It is important to note that comparative
62 studies have highlighted several human homologs involved in aging and neurodegenerative
63 disease in both *A. californica* and *L. stagnalis* (Fodor, Urban, Kemenes, Koene, & Pirger,
64 2020; Moroz et al., 2006; Moroz & Kohn, 2010), showing the great potential for future
65 molecular insights into brain aging and pathology using these unique mollusc models. More
66 importantly, a recent study has successfully established the use of CRISPR/Cas9 in *L.*
67 *stagnalis* embryos (Abe & Kuroda, 2019), further underscoring the high feasibility of *L.*
68 *stagnalis* for genetic studies.

69 Despite the importance of *L. stagnalis* to brain network, behaviour, and development studies,
70 genetic information is mostly limited to the identification and cloning of individual genes. Only
71 in the past decade have large-scale genomic analyses been put forward to characterize the

72 *L. stagnalis* transcriptome. For example, several studies (Bouetard et al., 2012; Davison &
73 Blaxter, 2005; Feng et al., 2009) have provided transcript sequencing data using expressed
74 sequence tags (EST) generated from *L. stagnalis* CNS libraries. Although these data have
75 provided valuable insights into partial gene expression, they were insufficient to perform
76 transcriptome analysis due to the limitation of the EST-based technique. A later study by
77 Sadamoto et al. in 2012 (Sadamoto et al., 2012) took advantage of the development of deep
78 RNA sequencing (RNA-Seq) techniques and performed de novo transcriptome shotgun
79 assembly (TSA) on *L. stagnalis* RNA samples of CNS. This study provided improved
80 transcriptome data with longer and larger sequences and also contributed to the identification
81 of novel transcripts in *L. stagnalis* CNS compared to previous studies. Moreover, from both
82 Blast searches in public databases and comparison with previous *L. stagnalis* and *A.*
83 *californica* EST, they showed that very few of their sequences had blast hits. This result was
84 mainly attributed to the lack of sufficient molluscan sequence coverage in the public
85 databases for valid dataset comparison, urging the need for continued genetic studies of *L.*
86 *stagnalis* and other gastropods. A very recent effort by Dong et al. (Dong et al., 2021) has
87 established an updated *L. stagnalis* transcriptome of adult CNS by RNA-Seq. However, the
88 above studies have focused on only one developmental time point, predominantly in adults.
89 Considering the increasing use of *L. stagnalis* for brain aging and pathology research (Fodor,
90 Urban, et al., 2020), updated transcriptome datasets and gene annotations including old or
91 aging snail CNS are critically needed.

92 Brain development, maturation, and aging are influenced by both intrinsic (genetic) and
93 extrinsic (environmental) factors throughout the life span of animals and human. Large-scale
94 study of transcriptional changes in brains of animals at various ages provide important
95 molecular insights into brain development, aging, pathology, and evolution. Spatial and/or
96 temporal transcriptome analyses of brains and other tissues have been carried out in human
97 (Kang et al., 2011; Tebbenkamp, Willsey, State, & Sestan, 2014), rats (Shavlakadze et al.,
98 2019), mice (Chou et al., 2016), chicken (Xu et al., 2018), zebrafish (Vesterlund, Jiao,
99 Unneberg, Hovatta, & Kere, 2011), and birds (Frias-Soler, Pildain, Parau, Wink, & Bairlein,
100 2020) among others. All these studies have contributed to our understanding of the
101 molecular basis of brain development. Invertebrates have also been utilized for study of
102 development and aging. Developmental transcriptomes of well-established invertebrate
103 models such as *Caenorhabditis elegans* (*C. elegans*) (Boeck et al., 2016; Lu, Lai, Liao, &
104 Tsai, 2020) and *Drosophila melanogaster* (*D. melanogaster*) (Graveley et al., 2011) have
105 been reported. Recent efforts have also focused on the transcriptome of aging *D.*
106 *melanogaster* (Moskalev et al., 2019; Pacifico, MacMullen, Walkinshaw, Zhang, & Davis,
107 2018) and *C. elegans* (Tarkhov et al., 2019), aiming to reveal molecular mechanisms of
108 longevity or aging trajectories.

109 In mollusca, the developmental (embryonic, larval, and metamorphic) transcriptome of *A.*
110 *californica* (Heyland, Vue, Voolstra, Medina, & Moroz, 2011) and maternal (1 to 2 cell and
111 ~32 cell) transcriptome of *L. stagnalis* have been conducted (Liu, Davey, Jackson, Blaxter, &
112 Davison, 2014). These studies shed novel insights into conserved sets of genes and
113 pathways in early development. However, these studies failed to inform how these genes or
114 other sets of genes are regulated in later stages of life, such as after animals are fully
115 matured and aged. Although whole-transcriptome changes in tail-withdrawal sensory
116 neurons of sexually matured and aged *A. californica* have been reported (Greer, Schmale, &
117 Fieber, 2018), transcriptome changes of entire CNS in young, mature, and aged *A.*
118 *californica* and *L. stagnalis* have not been carried out. Such studies are critical for our
119 complete understanding and comparative studies of age- or species- specific molecular
120 strategies that are key to the evolution, survival, and function of both invertebrate and
121 vertebrate.

122 To this end, in the present study, we provide whole transcriptome analysis in *L. stagnalis*
123 CNS from three different ages: 3 months (young), 6 months (adult), and 18 months (old).
124 This is the first time that changes in CNS transcriptome profiling during brain development,
125 maturation, and aging in *L. stagnalis* are analyzed. *L. stagnalis* has a relatively short life
126 cycle, with a life expectancy of about 1.5 to 3 years (Hermann et al., 2007). The embryonic
127 stage of the snail lasts for around two weeks, and eggs are contained in gelatinous masses
128 that are accessible for genetic manipulation. After hatching, young snails reach sexual
129 maturity at around 4 to 6 months of age, and senescence starts after 7-8 months (Hermann
130 et al., 2007; Janse, Slob, Popelier, & Vogelaar, 1988). Therefore, the 3-month-old age in our
131 study represents a rapid developing and sexual immature stage, the 6-month-old age
132 represents a fully, sexually mature stage, and 18-month-old represents an aging stage
133 (Hermann et al., 2007; Janse et al., 1988).

134 Using the above three age cohorts, our study generated 55-69 millions of 150 bp paired-end
135 RNA-Seq reads using the Illumina NovaSeq 6000 platform. Of these reads, ~74% were
136 successfully mapped to the unannotated reference genome of *L. stagnalis*. Our reference-
137 based transcriptome assembly yielded 42,478 gene loci, of which 37,661 genes encode
138 coding sequences (CDS) of at least 100 codons. In addition, we provide gene annotations for
139 32,288 out of 37,661 (~88%) of these sequences, contributing the largest number of
140 annotated genes in *L. stagnalis* CNS so far. Moreover, among 242 previously cloned *L.*
141 *stagnalis* genes, we were able to match ~87% of them in our transcriptome, a high
142 percentage of gene coverage. The changes in gene transcription levels were validated by
143 real-time qPCR for three *innexin* genes: *Inx1*, *Inx4* and *Inx5*. Lastly, our transcriptomic
144 analyses revealed distinct, age-specific gene clusters, differentially expressed genes, and
145 enriched pathways in young, adult, and old CNS. Together, these datasets are the largest
146 and most updated *L. stagnalis* CNS transcriptomes, which will serve as a resource for future
147 molecular studies and functional annotation of transcripts and genes in *L. stagnalis*.

148

149 **Materials and Methods**

150 **Animals and brain dissection**

151 *L. stagnalis* were maintained in artificial pond water at 20°C in a 12-hour light/dark cycle and
152 fed with romaine lettuce twice a week. *L. stagnalis* were obtained from the University of
153 Calgary, Canada (original stock was from the Vrije University in Amsterdam) and raised and
154 maintained in aquaria at Saint Louis University since 2015 according to protocols developed
155 and optimized as described previously (Mersman et al., 2020; Steen, Jager, & Hoven, 1968).
156 All procedures are in accordance with the standard operating protocol guidelines established
157 by the U.S. Department of Agriculture Animal and Plant Health Inspection Service. Animals
158 at 3 months old (young), 6 months old (adult) or 18 months old (old) were used for RNA
159 sequencing and qPCR. We used replicate samples for each developmental age, and for
160 each sample, the CNS of ten animals were pooled. The snails were de-shelled and
161 anesthetized in 10% (v/v) Listerine in *L. stagnalis* saline (51.3 mM NaCl; 1.7 mM KCl; 4.0
162 mM CaCl₂; 1.5 mM MgCl₂, 10 mM HEPES, pH 7.9), and the dissected central ring ganglia
163 were used for both RNA sequencing and qPCR.

164 **RNA extraction**

165 RNA was extracted from dissected *L. stagnalis* central ring ganglia using the RNeasy Mini Kit
166 (Qiagen, 74104) following the manufacturer's instructions. RNA concentration was assessed
167 using a Nanodrop 2000 Spectrophotometer (ThermoFisher, ND-2000). After RNA extraction,
168 genomic DNA (gDNA) was removed via the TURBO DNA-free kit (Invitrogen, AM1907).

169 **RNA sequencing library construction, sequencing, alignment, and transcriptome** 170 **assembly**

171 The construction of RNA sequencing libraries using polyA enrichment method was
172 performed by Novogene Corporation Inc (Sacramento, CA, USA). These libraries were
173 sequenced using the Illumina NovaSeq 6000 platform (Paired-end, 150 bp, insert size 250-
174 300 bp). The sequencing reads of each RNA-Seq library were aligned to the reference
175 genome of *L. stagnalis* (assembly v1.0 GCA_900036025.1) using HISAT2 (Kim, Langmead,
176 & Salzberg, 2015). The soft clipping option in HISAT2 was enabled to exclude low-quality
177 bases at both ends of reads. The number of reads in each sample successfully mapped to
178 the *L. stagnalis* reference genome are provided in **Supplemental table 1**. We used Stringtie
179 (Pertea et al., 2015) to assemble transcripts based on aligned reads. The expression
180 abundance of each transcript was quantified as fragment per kilobase million reads (FPKM).
181 The results of principal component analyses (PCA) of the abundance of transcripts (FPKM)
182 for all genes from all samples are provided in **Supplemental Fig. 1A**. The correlations of
183 gene expression profile between each pair of samples are provided in **Supplemental Fig.**
184 **1B**. The raw sequencing data generated in this study have been submitted to the NCBI
185 BioProject database under accession number PRJNA698985.

186 **Functional annotation of inferred *L. stagnalis* genes**

187 We first used TransDecoder v5.5.0 (Haas et al., 2013) to retrieve CDS and amino acid
188 sequences for each assembled transcript from the *L. stagnalis* reference genome based on
189 the merged annotation file generated by Stringtie. We applied two different methods to
190 annotate inferred *L. stagnalis* genes and combined the annotated information. The first
191 method was based on BLASTP searches against NCBI RefSeq amino acid sequences of
192 nine species closely related to *L. stagnalis*. These species included: *Biomphalaria glabrata*,
193 *Aplysia californica*, *Lottia gigantea*, *Pomacea canaliculata*, *Octopus bimaculoides*, *Octopus*
194 *vulgaris*, *Crassostrea virginica*, *Crassostrea gigas*, and *Mizuhopecten yessoensis*. The
195 second method was to search for the presence of Pfam domains in the inferred *L. stagnalis*
196 amino acid sequences using the “hmmscan” tool in HMMER3 (Mistry, Finn, Eddy, Bateman,
197 & Punta, 2013). The BLASTP and Pfam search results were integrated into the annotation of
198 predicted *L. stagnalis* open reading frames (ORFs) using TransDecoder-v5.5.0 (Haas et al.,
199 2013).

200 **Gene Ontology annotation of inferred genes in *L. stagnalis***

201 We used predicted protein sequences of *L. stagnalis* with at least 100 amino acids for Gene
202 Ontology (GO) annotation using Blast2GO (Conesa et al., 2005). This annotation analysis
203 was based on homology searches against the Mollusca phylum, *Caenorhabditis elegans*,
204 *Drosophila melanogaster*, and *Homo sapiens* using the latest reference protein database
205 (refseq_protein v5). We used an e-value threshold of 1.0E-3, top 20 blast hits, word size 6,
206 and HSP length cut-off of 33. GO annotation was based on the latest GO version (2020.06).
207 For GO enrichment analysis, Fisher’s exact test was used in combination with a False
208 Discovery Rate (FDR) correction for multiple testing (FDR < 0.05). R (Team, 2017) package
209 ggplot2 was used to plot results of GO enrichment analysis.

210 **Identification of previously cloned genes in *L. stagnalis***

211 We searched for previously cloned genes in *L. stagnalis* from the NCBI nucleotide database
212 (as of January 2021) to evaluate the completeness of our transcriptome assembly. Only
213 cloned genes that were supported by published studies were selected. The list of previously
214 cloned genes in *L. stagnalis* (NCBI ID, gene names and references) is provided in
215 **Supplemental Table 2**.

216 **Differential gene expression analysis and validation of gene expression by real-time** 217 **qPCR**

218 Differential expression (DE) analysis was carried out using DESeq2 (Love, Huber, & Anders,
219 2014) based on raw read counts retrieved by the featureCounts package of Subread v1.5.0
220 (Liao, Smyth, & Shi, 2014). The results of DE analysis by DESeq2 are shown in
221 **Supplemental file 1**.

222 We validated the differential gene expression through real-time quantitative polymerase
223 chain reactions (RT-qPCR). cDNA synthesis was performed from gDNA-removed RNA
224 samples using SuperScript IV VILO Master Mix (Invitrogen, 11766050) following the
225 manufacturer's instructions. SYBR Green PCR Master Mix (Applied Biosystems, 4309155)
226 was used for RT-qPCR in a QuantStudio 5 Real-Time PCR System (ThermoFisher). Primers
227 are listed in **Supplemental Table 3**. Primer set efficiency values ranged from 95.85-
228 104.26%, and R^2 values were 0.9807-0.9999. Two negative controls were used: qPCR
229 without reverse transcription and no template controls. Relative gene expression was
230 normalized to reference gene *β -tubulin*. The final qPCR product was also sequenced to
231 ensure the correct *innexin* paralog was amplified.

232 Because of the wide range of primer efficiencies, relative gene expression was calculated via
233 the Common Base Method (Ganger, Dietz, & Ewing, 2017) and normalized to reference
234 gene *β -tubulin*. Analysis of variance (ANOVA) was used to determine statistically significant
235 differences in gene expression at $p < 0.05$, and Tukey's HSD *Post-hoc* test was used when
236 appropriate.
237

238 **Results**

239 ***L. stagnalis* CNS transcriptome sequencing, assembly and gene annotation**

240 RNA-Seq was performed using CNS samples from young (3 months old), adult (6 months
241 old), and old (18 months old) snails (**Figure 1A**), with four biological replicates in each group
242 and ten snails in each replicate. Our RNA-Seq data provides a good sequencing depth, with
243 a total number of reads ranging from 55,601,129 (56M) to 69,121,300 (69M). The average
244 overall alignment rate is ~74% (**Supplemental Table 4**). A total of 61,994 transcripts from
245 42,478 genes are identified. 37,661 of those genes encode for proteins of at least 100 amino
246 acids. To provide functional annotations for inferred *L. stagnalis* genes, we retrieved
247 proteomic sequences of nine molluscan species from the NCBI RefSeq database (See
248 Materials and Methods). Our transcript assembly and gene function annotation provide the
249 first genome annotation for *L. stagnalis* (provided as **Supplemental file 2** in gff3 format).

250 **Transcriptional clustering pattern in CNS of young, adult, and old *L. stagnalis***

251 Our principal component analysis (PCA) of the 12 transcriptomes (three age groups, four
252 replication samples per age group) form three major clusters (**Supplemental Figure 1A**),
253 corresponding to the three age groups of samples. The majority of biological replicates
254 cluster together, suggesting that expression profiles are more similar in animals belonging to
255 the same-age cohort. The first principal component (PC1), which accounts for 68.12% of the
256 variance in the data, provides separation between young and the other two groups (adult and
257 old). The second principal component (PC2) only accounts for 7% of the variance, serving as
258 a discriminator between adult and old transcriptomes. These patterns suggest that there are
259 constitutive differences in transcriptomes between young and adult/old CNS, while adult and
260 old CNS transcriptomes are more similar to each other. These results are consistent with
261 pairwise Pearson correlations between these samples (**Supplemental Figure 1B**).

262 To identify genes that are differentially expressed (DE) during the development of the CNS,
263 we conducted pairwise comparisons of transcriptomes for the three groups of samples:
264 young vs. adult, young vs. old, and adult vs. old. We identify 20,141 significant DE genes
265 between young and adult groups; 18,394 DE genes between young and old groups; and only
266 3,108 significant DE genes between adult and old groups (FDR adjusted p -value $p < 0.05$;
267 \log_2 fold change $> |1|$) (**Figure 1B,C**). Interestingly, only 455 DE genes are present in all
268 comparisons. Together, these analyses suggest that most changes in CNS development
269 occur pronouncedly during transitions from young to adult, and less changes occur during
270 transitions from adult to old.

271 **Analysis of the DE genes confirms distinct gene expression patterns in young, adult, 272 and old *L. stagnalis***

273 Next, we selected the genes that are the most DE, based on their adjusted p -values in each
274 pairwise comparison. We first sorted the top 100 DE genes and then further refined by
275 selecting only the sequences with at least 100 codons; a total of 143 most DE genes are
276 used. Heatmap analysis of FPKM expression shows a different expression pattern among
277 age groups (**Figures 1D,E**). Specifically, consistent with the above principal component
278 analysis, individual replicates exhibit very similar regulation patterns within the same age
279 cohort (**Figure 1D**). Overall, the adult animal transcriptome shows more highly expressed
280 genes, while around half of genes in young and the majority of genes in old exhibit low
281 expression. The heatmap pattern also shows that 1) most genes with low expression in
282 young animals are highly expressed in adult and remain high in old; 2) most highly
283 expressed genes in young animals have low expression in adult and become further down-
284 regulated in old animals; 3) only a few clusters contain genes whose expression increases
285 from young to adult and then decreases from adult to old (**Figure 1D**). We also looked at the
286 top 2,000 genes with the highest variance across all samples. The heatmap in **Figure 1E**
287 shows 1) variance in DE gene expression, again, separates young transcriptome from
288 transcriptomes of adult and old, and the highest variance occurs in the young animal
289 transcriptome; 2) two big clusters of genes increase in expression from young to adult CNS
290 transcriptome and retain relatively high expression in old; 3) two big clusters of genes
291 decrease in expression from young to adult CNS transcriptome and further lower their
292 expression in old; 3) a few small clusters of genes increase expression from young to adult
293 and then decrease from adult to old. Together, these data indicate that there are distinct
294 changes of transcript profiling across life stages of animals. Next, we sought to study what
295 sets of DE genes and related pathways are involved in the expression patterns across
296 different life stages.

297 **Gene ontology analysis**

298 We performed GO annotation with Blast2Go (Conesa et al., 2005) for the 37,661 transcripts
299 that encode proteins with at least 100 amino acids (see Materials and Methods). A total of
300 32,288 transcripts (or genes) were successfully annotated with GO terms. GO enrichment
301 analysis was performed for DE genes in: all pairwise comparisons (455 genes), young
302 compared to adult CNS transcriptome (20,141), young compared to old CNS transcriptome
303 (18,394), and adult compared to old CNS transcriptome (3,108) (**Figure 2**). The enriched GO
304 terms of DE genes in all pairwise comparisons include biological processes that are related
305 to metabolism of nitrogen compounds, organic substances, macromolecules, and cellular
306 macromolecules. As expected from the huge overlap among significant DE genes, GO
307 enrichment from young compared to adult and young compared to old groups partially
308 overlap. In these two comparisons, the common GO terms in biological process are related
309 to gene expression (transcription by RNA polymerase II and positive or negative regulation of
310 gene expression). GO terms in cellular components are related to mitochondrial and

311 ribosome pathways (mitochondrial ribosome, mitochondrial matrix, mitochondrial membrane,
312 cytosolic ribosome, and ribonucleoprotein complex). Finally, GO terms in molecular function
313 are related to signalling receptor and signalling transduction pathways (signalling receptor
314 activity, G protein-coupled receptor activity, and transmembrane signalling receptor activity)
315 (**Figure 2**). The common enriched metabolic, mitochondrial, and ribosomal pathways
316 suggest that transcripts engaged in cellular metabolic, energy production, and protein
317 synthesis activity are actively regulated in the CNS of snails.

318 To gain further insights into what specific sets of DE genes are changed from young to adult
319 to old snail CNS, we analysed the FPKM expression of the top100 DE genes used in Figure
320 2D and examined their associated GO terms. A complete list of genes, their FPKM,
321 descriptions, and GO terms are provided in **Supplemental table 5**. We found that genes
322 significantly increased from young to adult and remain elevated in old animals, including
323 those involved in receptor signalling activity (e.g. N-methyl-D-aspartate receptor NR1 and
324 NR2, Mollusc insulin-related peptide MIP, and Notch 3 receptors), signalling transduction
325 mechanism (serine/threonine protein kinase TAO1-like TAOK1, protein kinase A PKA, and
326 serine/threonine-protein phosphatase 2A PIPA), synaptic vesicle proteins (e.g.
327 synaptotagmin1 and 4), ion channels (e.g. voltage-gated K⁺ channels Kv2.1a KCNB1),
328 metabolism (pyruvate kinase PKM-like isoform X3 PKM and phosphopractokinase-like
329 PFKM), membrane/membrane bound organelles (e.g. reticulon-3-A like and fat cadherin),
330 transcription and translation (poly [ADP-ribose] polymerase 14-like gene PARP and
331 translation initiation factor eIF-2 EIF2B4), and peptides and peptide enzymes (Titin-like X2
332 TTN and Peptidase C1-like). Interestingly, there are only a few DE genes that are
333 significantly increased from adult to old animals. These include
334 monooxygenase/oxidoreductase active (CYP2U1), cysteine dioxygenase type (CD01), and
335 endoglucanase E-4 like and A-like. Genes that are highly expressed in young and then
336 significantly decrease in adult and old animals include ECM structure constituents (e.g.
337 collagen 2A1, collagen 1A1, and fibril-forming collagen 2-chatin like). When comparing
338 expression of genes in adult and old, we found that most genes exhibit significantly lower
339 expression in old animals. These include stress and immune factors (dual oxidase 2-like
340 DUOX2, oxidase activity cytochrome P450 CYP10, suppressor of cytokine signalling 2
341 SOCS2, and heat shock protein 60 HSP 60), Ca²⁺ binding (Ca²⁺/CaM-serine kinase CASK),
342 protein ubiquitin (Myc binding protein MYCBP2 and ubiquitin-protein ligase E3A), and
343 membrane and cellular entity (cadherin, adhesion G-protein coupled receptor L2 like
344 GPCRL2, and disintegrin). Several above mentioned, stress-related genes and their
345 expressions (FPKM) in young, adult, and old *L. stagnalis* CNS are shown in **Supplemental**
346 **Figure 2**.

347 **qPCR studies confirm differential gene expression identified by RNA-Seq data**

348 We next performed qPCR to validate gene expression revealed by RNA-Seq by taking
349 advantage of our ongoing projects studying *L. stagnalis* gap junction *innexin* expression
350 (Mersman et al., 2020). *Innexin* is the invertebrate analogue for the vertebrate *connexin*, both
351 of which code for gap junction-forming proteins. Gap junctions are intercellular channels
352 essential for direct and synchronized communication among cells (Ovsepian, 2017). Our
353 transcriptome data detected three of the previously cloned *L. stagnalis innexin* genes: *Inx1*,
354 *Inx4*, and *Inx5*. FPKM data showed that *Inx1* is the most abundant gene, followed by *Inx4*,
355 and then *Inx5* in the CNS. The expression of these genes are upregulated in adult CNS and
356 then maintain a comparable level in old CNS (**Figure 3A**). In order to compare the gene
357 expression from our RNA-Seq data, we performed real-time qPCR from brain samples of
358 young, adult, or old snails. As shown in **Figure 3A,B**, both RNA sequencing data and qPCR
359 data show a similar pattern of expression over ages for each gene. More specifically, *Inx1*

360 has a significantly lower expression level in young animals compared to adult and old (RNA-
361 Seq FDR adjusted p -value young vs adult $p = 5.95 \times 10^{-7}$, young vs old $p = 3.73 \times 10^{-6}$; qPCR
362 Turkey's post-hoc test young vs adult $p = 0.001$ young vs old $p = 0.009$). *Inx4* also has
363 similar trends in gene expression in both RNA-Seq and qPCR, but it is expressed
364 significantly lower in the young animals only in the qPCR data, likely due to the increased
365 sensitivity of the qPCR technique than RNA-Seq (RNA-Seq FDR adjusted p -value young vs
366 adult $p = 0.391$, young vs old $p = 0.395$; qPCR Turkey's post-hoc test young vs adult $p =$
367 0.003 , young vs old $p = 0.003$). Finally, *Inx5* expression is also significantly lower in young
368 snails compared to adult and old (RNA-Seq FDR adjusted p -value young vs adult $p =$
369 2.42×10^{-11} , young vs old $p = 0.000$; qPCR Turkey's post-hoc test young vs adult $p = 0.001$,
370 young vs old $p = 0.002$). The concordance between RNA-Seq transcriptome expression and
371 qPCR confirms the reliability of our RNA-Seq measurements.

372 ***L. stagnalis* transcriptome assembly is further supported by the high coverage of** 373 **other previously cloned genes**

374 To further evaluate the quality and completeness of the transcriptome assembly, we tested
375 the coverage of previously cloned genes from *L. stagnalis* in our transcriptome. According to
376 the most recent NCBI nucleotide database, a total of 242 *L. stagnalis* genes have been
377 previously cloned (**Supplemental Table 2**). There are 210 of these genes (87%) present in
378 our transcriptome assembly, supporting that our transcriptome assembly from CNS samples
379 cover most of the previously known protein-coding genes in *L. stagnalis*. Considering that
380 only a portion of genes are expressed in brain tissues, it is expected that some previously
381 cloned genes would not be detected by this RNA-Seq study.

382 We investigated the previously cloned genes among the aforementioned GO terms. We can
383 find almost all of the previously cloned *L. stagnalis* acetylcholine receptor subunits (LnAChR)
384 among the enriched signalling GO terms. Of the twelve previously cloned subunits, we found
385 ten in our transcriptome. We further show that in the CNS transcriptome of adult and old
386 snails, the LnAChR subunits H and F have the highest expression (van Nierop et al., 2006).
387 Interestingly, in the CNS transcriptome of young snails, subunit G has the highest expression
388 (**Figure 4A**). These data seem to suggest changes in LnAChR composition during CNS
389 development. Moreover, two other synaptic receptors, the N-Methyl-D-aspartic acid receptor
390 (NMDAR) and the serotonin receptor (5-HT receptor) have a significantly lower expression in
391 the young compared to adult and old CNS transcriptomes (NMDAR: RNA-Seq FDR adjusted
392 p -value young vs adult $p = 6.35 \times 10^{-16}$, young vs old $p = 3.08 \times 10^{-17}$; 5-HT receptor: RNA-Seq
393 FDR adjusted p -value young vs adult $p = 9.90 \times 10^{-10}$, young vs old $p = 9.41 \times 10^{-5}$) (**Figure**
394 **4B**). These data further suggest that, similar to humans, CNS synaptic development lasts
395 after birth in snails, and a brain in a young individual is different from an adult or old brain,
396 not only in ultrastructure, but also in phenotypes and transcriptome expression.

397 Interestingly, of the known cloned genes matched in our transcriptome (210 genes), nine
398 genes have significant differential gene expression in all pairwise comparisons (young vs
399 adult, young vs old, adult vs old; **Figure 3A,B; Figure 5**). These include three genes coding
400 for the molluscan insulin peptide (MIP, LSTA.21646), the enzyme tryptophan hydroxylase
401 (LSTA.51), and the FMRFamide protein (LSTA.14894) that significantly increase in
402 expression from young to adult to old snails (**Table 1, Figure 5**). Two genes coding for
403 aquaporin channel protein (CoAQP1, LSTA.13986) and chitinase II (LSTA.17318) have an
404 inverse pattern with significantly decreasing gene expression from young to adult to old
405 animals (**Table 1, Figure 5**). Another three genes coding for a serum-dependent glutathione
406 peroxidase (LSTA.693), *innexin5* (*Inx5*, LSTA.18425, as previously shown in **Figure 3A**),
407 and another aquaporin channel protein (LsAQP1, LSTA.13985) are expressed higher in adult
408 snails compared to young and old (**Table 1, Figure 5**). Lastly, the gene coding for a voltage-

409 dependent L-type calcium channel alpha-1 subunit was highly expressed in young snails
410 compared to adult and old (**Table 1, Figure 5**).

411

412

413 *Table 1. Significantly differentially expressed cloned genes*

Gene	Locus ID	FPKM-Young	FPKM-Adult	FPKM-Old
MIP	LSTA.21646	978.861	6055.743	7515.437
tryptophan hydroxylase	LSTA.51	64.414	447.099	698.380
FMRFamide protein	LSTA.14894	686.373	1042.714	1357.454
CoAQP1	LSTA.13986	142.268	58.499	27.372
chitinase II	LSTA.17318	5.811	5.348	3.259
serum-dependent glutathione peroxidase	LSTA.693	2.669	31.388	18.185
Inx5	LSTA.18425	0.361	1.208	0.761
LsAQP1	LSTA.13985	115.796	176.112	69.177
voltage-dependent L-type calcium channel alpha-1 subunit	LSTA.19085	1.164	0.757	0.759

414

415 ***Genes involved in diseases are upregulated in the CNS transcriptome of adult and old***
416 ***animals***

417 Lastly, a recent paper using both *A. californica* and *L. stagnalis* has provided the cloned
418 sequences for several genes involved in neurodegenerative disorders like Huntington
419 disease, Parkinson's disease (PD), and Alzheimer's disease (AD) (Fodor, Urban, et al.,
420 2020). Identification and expression analysis of these genes in the *L. stagnalis* transcriptome
421 is promising for the use of *L. stagnalis* as a model for studying neurodegenerative diseases.
422 In our transcriptome, we discovered that the expression of these genes change with age.
423 More specifically, Parkinson's disease protein 7 (*PARK7*), huntingtin, choline
424 acetyltransferase, and presenilin genes are all upregulated in the CNS of adult and old
425 compared to young animals (**Supplemental Figure 3**).

426 In addition to these well-recognized genes, there are several other genes that are
427 upregulated in adult and old animals compared to young animals. These include Arginase 1
428 (*ARG1*, linked to many human diseases), reticulons (linked to AD and amyotrophic lateral
429 sclerosis) (Yang & Strittmatter, 2007), proton myo-inositol cotransporter (*SCL2A13*, linked to
430 AD) (Teranishi et al., 2015), Rab GDP dissociation inhibitor (linked to mental retardation)
431 (Ishizaki et al., 2000), and several tumor genes such as tumor protein D52 (*TPD 52*), tumor
432 suppressor gene e-cadherin like, and protein phosphatase2A (*PP2A*); a few of these genes
433 and their expressions in young, adult, and old *L. stagnalis* are shown in **Supplemental**
434 **Figure 3**). Expression of these disease-related genes in *L. stagnalis* provides a unique
435 opportunity for using *L. stagnalis* as a model system to study these genes.

436

437 **Discussion**

438 *L. stagnalis* has served as a unique model organism for the study of neural networks,
439 neuronal development, and synapse formation (Getz et al., 2018; Haque et al., 2006;
440 Swinton et al., 2019) due to its simple, well-characterized, and easily accessible CNS. In
441 addition, it has recently emerged as a useful model for studying brain aging and
442 neurodegenerative diseases (Fodor, Urban, et al., 2020; Hermann et al., 2020; Maasz et al.,
443 2017). Here, we generated datasets that allow for the first in-depth look at transcriptome
444 changes in gene expression of *L. stagnalis* CNS from young (3 month), adult (6 month), and
445 old (18 month) animals. Our study identifies new *L. stagnalis* sequences, with a good read
446 depth of up to 69 million total fragments (150 bp paired-end reads); moreover, we took
447 advantage of the Blast2GO bioinformatics platform to provide gene annotation and gene
448 ontology (GO) annotation for over 30,000 sequences. This study also reveals temporal
449 dynamics of transcriptional profiling and key DE genes/pathways in *L. stagnalis* CNS at
450 multiple time points of the animal's life span. Such information will be instrumental for future
451 age-related phenotypical analyses in single cells, neuronal networks, and whole animals.

452 Knowledge about age-associated transcript changes can improve our understanding of how
453 intrinsic profiling plays a role in influencing anatomical, physiological, and pathophysiological
454 properties in animals and human at different life stages. Transcriptomic analyses of human
455 brains at different ages have shown that the majority of protein-coding genes are
456 spatiotemporally regulated, and the transcriptional differences are most pronounced during
457 early development (Kang et al., 2011). Similarly, our data reveal that constitutive differences
458 in transcriptomes exist between young and adult CNS, while adult and old CNS exhibit fewer
459 differences in transcripts. In the rat hippocampus, 229 genes were reported to be linearly up-
460 or down-regulated across the lifespan of a healthy animal (Shavlakadze et al., 2019).
461 Previous studies of transcriptomic profiling of sensory neurons from *A. californica* at 8
462 (matured), and 12 (aged) months reported that half of the genes were up- and half of the
463 genes were down-regulated between the two cohorts of neurons (Greer et al., 2018). Our
464 data in this study demonstrates that in *L. stagnalis* CNS, there are genes exhibiting linear up-
465 or down-regulation from young to adult to old (Figure 1D), but there are also many genes that
466 are regulated in a non-linear manner. For example, some genes are upregulated from young
467 to adult and appear to either maintain a comparable level of expression or significantly
468 decreased expression in old animals as shown in **Figures 3-5** and **Supplemental Figure 2-3**.
469 The linear or non-linear expression of genes across animals at different ages and in
470 different species may highly correlate with age- and species-specific functions of these
471 genes. Interestingly, the principal component analysis revealed that the majority of *L.*
472 *stagnalis* (**Supplemental Figure 1**) biological replicates clustered together. The same
473 clustering pattern was found in *A. californica* (Greer et al., 2018) suggesting that individuals
474 of these two species in the same age group share similar transcript profiles. These results
475 suggest that age is an important, determinizing factor for transcriptional profiling between
476 individuals. Together, these data support that whole transcriptome comparison can serve as
477 a valuable tool for discovering age-specific genes, and these mollusc organisms could serve
478 as useful models for studying age-related molecular basics of brain development and aging.

479

480 Our gene ontology analyses indicate that the majority of DE genes occur between young and
481 adult CNS, and the DE genes are enriched in metabolic processes, gene expression, and
482 mitochondrial, ribosome, and signalling receptor pathways. This finding is consistent with a
483 recent study of adult *L. stagnalis* CNS transcriptome compared to several other adult
484 organisms used in neurobiology including *Mus musculus* (mouse), *Danio rerio* (zebrafish),
485 *Xenopus tropicalis*, *C. elegans*, and *D. melanogaster* (Dong et al., 2021). Specifically, this
486 study focused on the annotation of the top 20 expressed transcripts in these models. The

487 authors revealed an abundance of transcripts involved in energy production, protein
488 synthesis, and signalling transduction of adult CNS, indicating evolutionally conserved roles
489 of these pathways in mature adult animals of both invertebrates and vertebrates. Because of
490 the importance of these pathways in adult animals, it is not surprising that previous studies
491 have primarily focused on cloning genes involved in these pathways. Indeed, among many
492 cloned genes in our *L. stagnalis* transcriptome, we can detect DE genes encoding proteins
493 involved in these pathways. For example, our RNA-Seq data identified ten of the twelve *L.*
494 *stagnalis* LnAChR subunits that have been previously cloned and sequenced (van Nierop et
495 al., 2006). Interestingly, we provide evidence that these subunits are differentially expressed
496 in the snail's CNS at different ages: the subunit H is most highly expressed in adult and old,
497 followed by the F subunit, while the G subunit is most highly expressed in young snails. The
498 expression of LnAChR subunits in adult snails is consistent with literature showing that
499 subunits H and F together account for approximately half of LnAChR expression in the *L.*
500 *stagnalis* CNS as shown by *in situ* hybridization (ISH) (van Nierop et al., 2006). Studies in rat
501 brain have also shown that various nAChR subunits are expressed at different ages and in
502 different brain areas (Cimino et al., 1995; X. Zhang, Liu, Miao, Gong, & Nordberg, 1998).
503 Studies comparing primates and humans to rodent brains have shown that the expression of
504 nAChR subunits is conserved in some brain areas but not others (Zoli, Pistillo, & Gotti,
505 2015). Furthermore, molluscan and other invertebrate species are known to have not only
506 excitatory, sodium-selective nAChRs, but also inhibitory, chloride-selective nAChRs (van
507 Nierop et al., 2005). Considering the properties of cation or anion conductance of LnAChR
508 subunits, we can appreciate the importance of differential expression of these subunits
509 across the lifespan of *L. stagnalis* for maintaining excitability homeostasis. Specific
510 pharmacological properties have been demonstrated for nAChRs composed of different
511 subunits in both mammalian (Papke, Dwoskin, & Crooks, 2007; Zoli et al., 2015), and
512 invertebrate models (Lansdell, Collins, Goodchild, & Millar, 2012). Our transcriptome data
513 suggest that the expression pattern or properties of LnAChRs might be important in CNS
514 development and function. Therefore, it would be interesting to investigate the
515 pharmacological properties of the different LnAChR subunits and their spatiotemporal
516 expression and function in the CNS of *L. stagnalis* in the future.

517 Among other previously cloned neurotransmitter receptors, we found that the N-Methyl-D-
518 aspartic acid (NMDA) and the serotonin (5-HT) receptors are differentially expressed when
519 comparing the CNS of young and adult/old snails (**Figure 4B**). Studies in both human (Bar-
520 Shira, Maor, & Chechik, 2015; Law et al., 2003) and rat (Monyer, Burnashev, Laurie,
521 Sakmann, & Seeburg, 1994) have shown differential expression of the NMDAR subunits
522 NR1 and NR2 at different ages. Similarly, 5-HT receptors have been shown to be
523 differentially expressed during human early postnatal development and into adulthood (Bar-
524 Shira et al., 2015; Lambe, Fillman, Webster, & Shannon Weickert, 2011). Importantly,
525 aberrant expression and/or function of NMDA and 5-HT receptors have been associated with
526 neurodevelopmental disorders such as schizophrenia and autism (Carlsson, 1998; du Bois &
527 Huang, 2007; Ju & Cui, 2016; Seshadri, Klaus, Winkowski, Kanold, & Plenz, 2018; Sodhi &
528 Sanders-Bush, 2004; Xia et al., 2018). These changes in neurotransmitter receptor
529 expression at different ages suggest ongoing synaptic development or synaptic
530 diversification when *L. stagnalis* CNS progresses from young to a fully matured stage. The
531 significant up-regulation of genes encoding these transmitter receptors as well as
532 synaptotagmin, gap junctions, ion channels, FMRFamide and Mollusc insulin-related
533 peptides (**Supplemental Table 5** and results) clearly indicates the active engagement of
534 intercellular communication and synaptic plasticity in these adult animals. Transcript
535 regulation of synaptic genes may reflect animal behavioural changes; compared to young,
536 adult and old animals normally exhibit more vigorous and diverse behaviours including

537 reproduction, feeding, locomotion, respiration, and associative learning, for which the above-
538 mentioned synaptic machinery components play major roles (Dong et al., 2021; Ha, Kohn,
539 Bobkova, & Moroz, 2006; Hoek et al., 2005; Ito et al., 2012; Kojima et al., 2015; Mersman et
540 al., 2020; Murakami et al., 2013; Yeoman et al., 1994).

541 Neural communication relies on both the transmitter receptor-mediated chemical synapse
542 and the gap junction-mediated electrical synapse (Pereda, 2014); however, the latter is
543 severely understudied in *L. stagnalis* due to the lack of genetic information for gap junction
544 forming innexins. Recently, eight *innexin* genes, *Lst Inx1-Lst Inx 8*, have been sequenced
545 and cloned in *L. stagnalis* by our lab (Mersman et al., 2020). We mapped three of these
546 genes, *Lst Inx1*, *Lst Inx4*, and *Lst Inx5*, in our transcriptome data. The other *innexin* genes
547 might have expression levels that are too low to be measured in our transcriptome data, or
548 the genome assembly we used for gene mapping might have distributed those sequences on
549 different scaffolds. If we look at the three *innexin* genes that we were able to detect, both
550 transcriptome and RT-qPCR confirm differential expression at different ages (**Figure 3A-B**).
551 Studies in vertebrates have shown that specific connexin composition determines gap
552 junction channel properties (Beyer, Lipkind, Kyle, & Berthoud, 2012; Rackauskas,
553 Neverauskas, & Skeberdis, 2010). Moreover, a study in the invertebrate *D. melanogaster*
554 showed that two innexins, shakB and ogre, are not interchangeable, as they fail to rescue the
555 other's mutant (Curtin, Zhang, & Wyman, 2002). The differential expression of *innexin* genes
556 in *L. stagnalis* further suggests that gap junction channels formed by different innexin
557 proteins might have a specific role and are, hence, differentially expressed at different ages.

558 In addition to previously known genes, it is interesting to note a few unstudied genes in the *L.*
559 *stagnalis* transcriptome that exhibit age-specific expression patterns across life stages (as
560 described in results). For example, genes related to oxidative stress and immunity response
561 are either up- or down-regulated in old animals when compared to young and adult animals
562 (**Supplemental Figure 2**). These include cytochrome P450 (CYP2U1 and CYP10), dual
563 oxidase 2 (DUOX2), and suppressor of cytokine signalling 2 (SOCS2). The cytochromes
564 P450 (CYPs) constitute a large superfamily of heme proteins that are largely involved in the
565 oxidative metabolism of environmental (xenobiotics such as drugs and pesticides) or
566 endogenous (steroid hormones, fatty acid, etc) compounds (Dhers, Ducassou, Boucher, &
567 Mansuy, 2017; Montellano, 2015). Both CYP2U1 transcripts and proteins are widely
568 expressed in various brain regions of human and rats and are involved in the metabolism of
569 fatty acids and xenobiotics in the brain (Dhers et al., 2017). Interestingly, CYP10 has been
570 cloned in *L. stagnalis* and found to be abundantly expressed in the female gonadotropic
571 hormone producing dorsal bodies (Teunissen, Geraerts, van Heerikhuizen, Planta, & Joosse,
572 1992). DUOX are oxidoreductase enzymes that catalyse the synthesis of reactive oxygen
573 species (ROS) molecules including the anion superoxide (O_2^-) and hydrogen peroxide
574 (H_2O_2). DUOX as well as the previously cloned GPX (**Figure 5**) have recently been
575 demonstrated to be DE in *L. stagnalis* transcriptome in response to ecoimmunological
576 challenges (Seppala et al., 2021). SOC2 acts as a negative feedback inhibitor for a variety of
577 cytokine signalling in both vertebrates and invertebrates (Wang, Wangkahart, Secombes, &
578 Wang, 2019; Y. Zhang et al., 2010). Because of the significant regulation of these oxidative
579 stress and immune defense genes across life stages, it is critical to study their roles in animal
580 health, aging, and diseases in future studies.

581

582 Finally, our transcriptomic data also revealed changes in disease-relevant genes associated
583 with neurodegeneration, aging, and cancer, thus affording a unique opportunity to study
584 cellular and molecular functions of these genes by taking advantage of the simplicity of *L.*
585 *stagnalis* CNS. In addition, sequenced homologs of several genes known to be involved in

586 aging and neurodegenerative disease (e.g. Parkinson's disease protein 7 (*PARK7*),
587 huntingtin, presenilin1, and choline acetyltransferase (AChAT) (Fodor, Urban, et al., 2020),
588 among others) have recently become available. Our data reveals that in *L. stagnalis*, the
589 expression of these genes is upregulated in adult and old CNS compared to young CNS. In
590 addition to these genes, in the present study, we have discovered several other disease-
591 related genes (Supplemental Table 5 and Supplemental Figure 3). Firstly, the membrane
592 proton myo-inositol cotransport (SLC2A13) increases expression in the CNS of adult and old
593 compared to young *L. stagnalis*. Similar to presenilin1, proton myo-inositol cotransport is
594 found to be a novel gamma-secretase associated protein that selectively regulates A β
595 production (Teranishi et al., 2015). Secondly, the present study reveals increased expression
596 of reticulons which have been linked to AD and amyotrophic lateral sclerosis (ALS) (Yang &
597 Strittmatter, 2007). Reticulons is a group of evolutionarily conserved proteins residing
598 predominantly in the endoplasmic reticulum that promote membrane curvature, vesicle
599 formation, and nuclear pore complex formation. Since all these proteins are potentially
600 related to AD, it would be interesting to investigate their roles in learning and memory or
601 aging in future studies. While mutation, deletion, or decrease in expression of these disease-
602 related genes are the primary cause of diseases (Bird, Stranahan, Sumi, & Raskind, 1983;
603 Domingo & Klein, 2018; Nance, 2017; Nikolac Perkovic & Pivac, 2019), the purpose for
604 maintaining a high expression of these gene transcripts in the CNS of adult and old animals
605 is not known. However, our results may partially indicate that the abundant expression of
606 these disease-related genes could be a result of normal physiological requirements or the
607 natural aging process of mollusc CNS.

608

609 **Conclusions**

610 Overall, our RNA-seq study provided a much-needed *L. stagnalis* transcriptome assembly,
611 with gene and GO annotation for more than 30,000 predicted genes. Furthermore, the
612 analysis of CNS from different ages demonstrates the importance of this model for
613 uncovering molecular insights in young, adult, and old life stages. This dataset will be useful
614 for future discoveries of genes, expression profiling, and signalling pathways in different ages
615 of animals. It also serves as a helpful resource for future annotation of genes and the
616 genome of *L. stagnalis*.

617

618

619 **Acknowledgement**

620 This work was supported by the National Science Foundation (1916563) and the Saint Louis
621 University Start-up Fund awarded to Dr. Xu.

622

623 **Competing interests**

624 The authors declare no competing and financial interests.

625

626 **References**

627

- 628 Abe, M., & Kuroda, R. (2019). The development of CRISPR for a mollusc establishes the formin *Lsdia1*
629 as the long-sought gene for snail dextral/sinistral coiling. *Development*, *146*(9).
630 doi:10.1242/dev.175976
- 631 Arundell, M., Patel, B. A., Straub, V., Allen, M. C., Janse, C., O'Hare, D., . . . Yeoman, M. S. (2006).
632 Effects of age on feeding behavior and chemosensory processing in the pond snail, *Lymnaea*
633 *stagnalis*. *Neurobiol Aging*, *27*(12), 1880-1891. doi:10.1016/j.neurobiolaging.2005.09.040
- 634 Bar-Shira, O., Maor, R., & Chechik, G. (2015). Gene Expression Switching of Receptor Subunits in
635 Human Brain Development. *PLoS Comput Biol*, *11*(12), e1004559.
636 doi:10.1371/journal.pcbi.1004559
- 637 Beyer, E. C., Lipkind, G. M., Kyle, J. W., & Berthoud, V. M. (2012). Structural organization of
638 intercellular channels II. Amino terminal domain of the connexins: sequence, functional roles,
639 and structure. *Biochim Biophys Acta*, *1818*(8), 1823-1830.
640 doi:10.1016/j.bbamem.2011.10.011
- 641 Bird, T. D., Stranahan, S., Sumi, S. M., & Raskind, M. (1983). Alzheimer's disease: choline
642 acetyltransferase activity in brain tissue from clinical and pathological subgroups. *Ann*
643 *Neurol*, *14*(3), 284-293. doi:10.1002/ana.410140306
- 644 Boeck, M. E., Huynh, C., Gevirtzman, L., Thompson, O. A., Wang, G., Kasper, D. M., . . . Waterston, R.
645 H. (2016). The time-resolved transcriptome of *C. elegans*. *Genome Res*, *26*(10), 1441-1450.
646 doi:10.1101/gr.202663.115
- 647 Bouetard, A., Noirot, C., Besnard, A. L., Bouchez, O., Choisne, D., Robe, E., . . . Coutellec, M. A. (2012).
648 Pyrosequencing-based transcriptomic resources in the pond snail *Lymnaea stagnalis*, with a
649 focus on genes involved in molecular response to diquat-induced stress. *Ecotoxicology*, *21*(8),
650 2222-2234. doi:10.1007/s10646-012-0977-1
- 651 Carlsson, M. L. (1998). Hypothesis: is infantile autism a hypoglutamatergic disorder? Relevance of
652 glutamate - serotonin interactions for pharmacotherapy. *J Neural Transm (Vienna)*, *105*(4-5),
653 525-535. doi:10.1007/s007020050076
- 654 Chou, S. J., Wang, C., Sintupisut, N., Niou, Z. X., Lin, C. H., Li, K. C., & Yeang, C. H. (2016). Analysis of
655 spatial-temporal gene expression patterns reveals dynamics and regionalization in
656 developing mouse brain. *Sci Rep*, *6*, 19274. doi:10.1038/srep19274
- 657 Cimino, M., Marini, P., Colombo, S., Andena, M., Cattabeni, F., Fornasari, D., & Clementi, F. (1995).
658 Expression of neuronal acetylcholine nicotinic receptor alpha 4 and beta 2 subunits during
659 postnatal development of the rat brain. *J Neural Transm Gen Sect*, *100*(2), 77-92.
660 doi:10.1007/BF01271531
- 661 Conesa, A., Gotz, S., Garcia-Gomez, J. M., Terol, J., Talon, M., & Robles, M. (2005). Blast2GO: a
662 universal tool for annotation, visualization and analysis in functional genomics research.
663 *Bioinformatics*, *21*(18), 3674-3676. doi:10.1093/bioinformatics/bti610
- 664 Curtin, K. D., Zhang, Z., & Wyman, R. J. (2002). Gap junction proteins are not interchangeable in
665 development of neural function in the *Drosophila* visual system. *J Cell Sci*, *115*(Pt 17), 3379-
666 3388.
- 667 Davison, A., & Blaxter, M. L. (2005). An expressed sequence tag survey of gene expression in the
668 pond snail *Lymnaea stagnalis*, an intermediate vector of trematodes [corrected].
669 *Parasitology*, *130*(Pt 5), 539-552. doi:10.1017/s0031182004006791
- 670 de Weerd, L., Hermann, P. M., & Wildering, W. C. (2017). Linking the 'why' and 'how' of ageing:
671 evidence for somatotropic control of long-term memory function in the pond snail *Lymnaea*
672 *stagnalis*. *J Exp Biol*, *220*(Pt 22), 4088-4094. doi:10.1242/jeb.167395
- 673 Dhers, L., Ducassou, L., Boucher, J. L., & Mansuy, D. (2017). Cytochrome P450 2U1, a very peculiar
674 member of the human P450s family. *Cell Mol Life Sci*, *74*(10), 1859-1869.
675 doi:10.1007/s00018-016-2443-3
- 676 Dodd, S., Rothwell, C. M., & Lukowiak, K. (2018). Strain-specific effects of crowding on long-term
677 memory formation in *Lymnaea*. *Comp Biochem Physiol A Mol Integr Physiol*, *222*, 43-51.
678 doi:10.1016/j.cbpa.2018.04.010

- 679 Domingo, A., & Klein, C. (2018). Genetics of Parkinson disease. *Handb Clin Neurol*, *147*, 211-227.
680 doi:10.1016/B978-0-444-63233-3.00014-2
- 681 Dong, N., Bandura, J., Zhang, Z., Wang, Y., Labadie, K., Noel, B., . . . Feng, Z. P. (2021). Ion channel
682 profiling of the *Lymnaea stagnalis* ganglia via transcriptome analysis. *BMC Genomics*, *22*(1),
683 18. doi:10.1186/s12864-020-07287-2
- 684 du Bois, T. M., & Huang, X. F. (2007). Early brain development disruption from NMDA receptor
685 hypofunction: relevance to schizophrenia. *Brain Res Rev*, *53*(2), 260-270.
686 doi:10.1016/j.brainresrev.2006.09.001
- 687 Feng, Z. P., Zhang, Z., van Kesteren, R. E., Straub, V. A., van Nierop, P., Jin, K., . . . Smit, A. B. (2009).
688 Transcriptome analysis of the central nervous system of the mollusc *Lymnaea stagnalis*. *BMC*
689 *Genomics*, *10*, 451. doi:10.1186/1471-2164-10-451
- 690 Fodor, I., Hussein, A. A., Benjamin, P. R., Koene, J. M., & Pirger, Z. (2020). The unlimited potential of
691 the great pond snail, *Lymnaea stagnalis*. *Elife*, *9*. doi:10.7554/eLife.56962
- 692 Fodor, I., Urban, P., Kemenes, G., Koene, J. M., & Pirger, Z. (2020). Aging and disease-relevant gene
693 products in the neuronal transcriptome of the great pond snail (*Lymnaea stagnalis*): a
694 potential model of aging, age-related memory loss, and neurodegenerative diseases. *Invert*
695 *Neurosci*, *20*(3), 9. doi:10.1007/s10158-020-00242-6
- 696 Ford, L., Crossley, M., Vadukul, D. M., Kemenes, G., & Serpell, L. C. (2017). Structure-dependent
697 effects of amyloid-beta on long-term memory in *Lymnaea stagnalis*. *FEBS Lett*, *591*(9), 1236-
698 1246. doi:10.1002/1873-3468.12633
- 699 Frias-Soler, R. C., Pildain, L. V., Parau, L. G., Wink, M., & Bairlein, F. (2020). Transcriptome signatures
700 in the brain of a migratory songbird. *Comp Biochem Physiol Part D Genomics Proteomics*, *34*,
701 100681. doi:10.1016/j.cbd.2020.100681
- 702 Ganger, M. T., Dietz, G. D., & Ewing, S. J. (2017). A common base method for analysis of qPCR data
703 and the application of simple blocking in qPCR experiments. *BMC Bioinformatics*, *18*(1), 534.
704 doi:10.1186/s12859-017-1949-5
- 705 Getz, A. M., Wijdenes, P., Riaz, S., & Syed, N. I. (2018). Uncovering the Cellular and Molecular
706 Mechanisms of Synapse Formation and Functional Specificity Using Central Neurons of
707 *Lymnaea stagnalis*. *ACS Chem Neurosci*, *9*(8), 1928-1938.
708 doi:10.1021/acschemneuro.7b00448
- 709 Graveley, B. R., Brooks, A. N., Carlson, J. W., Duff, M. O., Landolin, J. M., Yang, L., . . . Celniker, S. E.
710 (2011). The developmental transcriptome of *Drosophila melanogaster*. *Nature*, *471*(7339),
711 473-479. doi:10.1038/nature09715
- 712 Greer, J. B., Schmale, M. C., & Fieber, L. A. (2018). Whole-transcriptome changes in gene expression
713 accompany aging of sensory neurons in *Aplysia californica*. *BMC Genomics*, *19*(1), 529.
714 doi:10.1186/s12864-018-4909-1
- 715 Ha, T. J., Kohn, A. B., Bobkova, Y. V., & Moroz, L. L. (2006). Molecular characterization of NMDA-like
716 receptors in *Aplysia* and *Lymnaea*: relevance to memory mechanisms. *Biol Bull*, *210*(3), 255-
717 270. doi:10.2307/4134562
- 718 Haas, B. J., Papanicolaou, A., Yassour, M., Grabherr, M., Blood, P. D., Bowden, J., . . . Regev, A. (2013).
719 De novo transcript sequence reconstruction from RNA-seq using the Trinity platform for
720 reference generation and analysis. *Nat Protoc*, *8*(8), 1494-1512. doi:10.1038/nprot.2013.084
- 721 Haque, Z., Lee, T. K., Inoue, T., Luk, C., Hasan, S. U., Lukowiak, K., & Syed, N. I. (2006). An identified
722 central pattern-generating neuron co-ordinates sensory-motor components of respiratory
723 behavior in *Lymnaea*. *Eur J Neurosci*, *23*(1), 94-104. doi:10.1111/j.1460-9568.2005.04543.x
- 724 Hermann, P. M., de Lange, R. P., Pieneman, A. W., ter Maat, A., & Jansen, R. F. (1997). Role of
725 neuropeptides encoded on CDCH-1 gene in the organization of egg-laying behavior in the
726 pond snail, *Lymnaea stagnalis*. *J Neurophysiol*, *78*(6), 2859-2869.
727 doi:10.1152/jn.1997.78.6.2859
- 728 Hermann, P. M., Lee, A., Hulliger, S., Minvielle, M., Ma, B., & Wildering, W. C. (2007). Impairment of
729 long-term associative memory in aging snails (*Lymnaea stagnalis*). *Behav Neurosci*, *121*(6),
730 1400-1414. doi:10.1037/0735-7044.121.6.1400

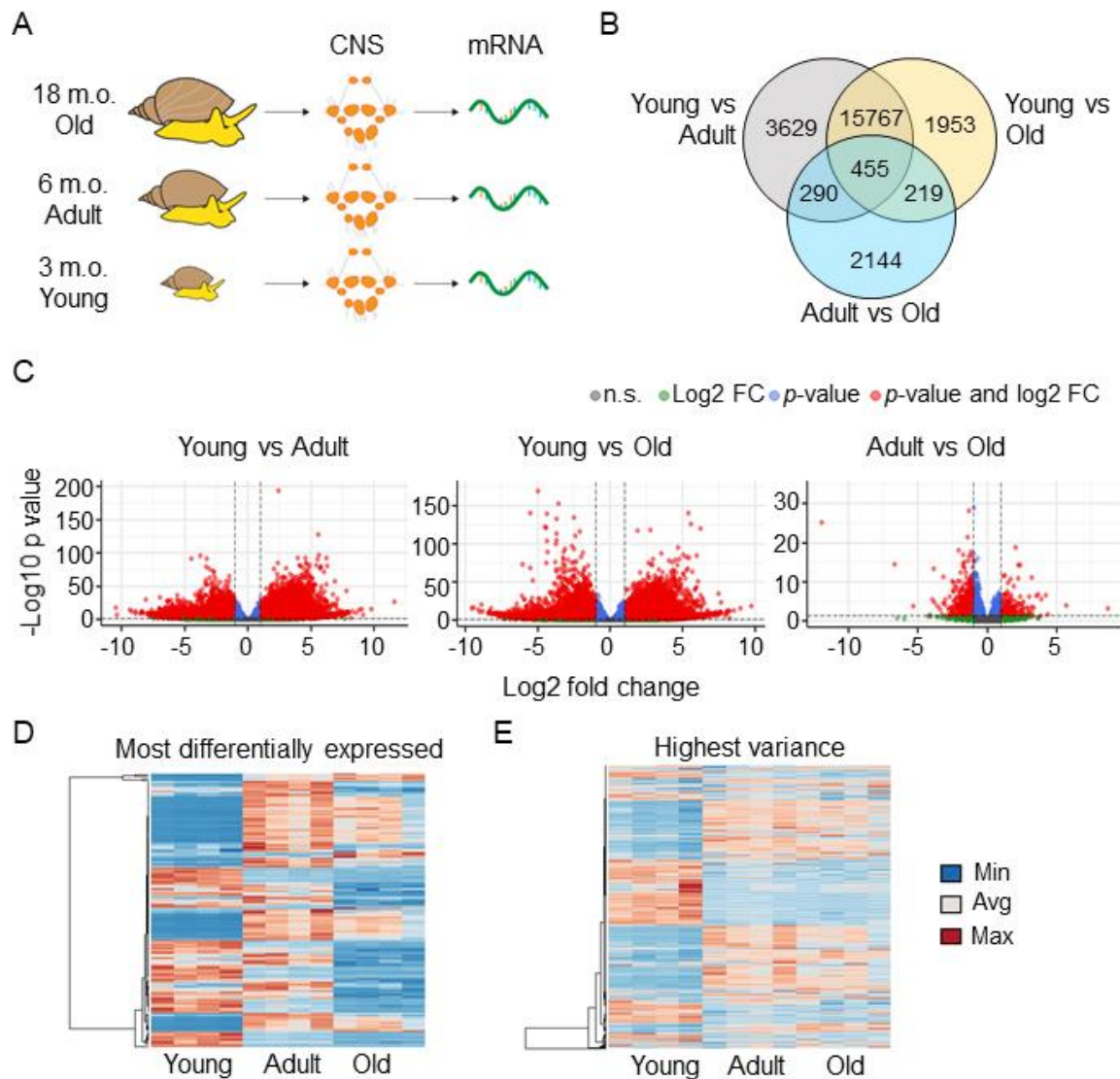
- 731 Hermann, P. M., Perry, A. C., Hamad, I., & Wildering, W. C. (2020). Physiological and pharmacological
732 characterization of a molluscan neuronal efflux transporter; evidence for age-related
733 transporter impairment. *J Exp Biol*, 223(Pt 2). doi:10.1242/jeb.213785
- 734 Heyland, A., Vue, Z., Voolstra, C. R., Medina, M., & Moroz, L. L. (2011). Developmental transcriptome
735 of *Aplysia californica*. *J Exp Zool B Mol Dev Evol*, 316B(2), 113-134. doi:10.1002/jez.b.21383
- 736 Hoek, R. M., Li, K. W., van Minnen, J., Lodder, J. C., de Jong-Brink, M., Smit, A. B., & van Kesteren, R.
737 E. (2005). LFRFamides: a novel family of parasitism-induced -RFamide neuropeptides that
738 inhibit the activity of neuroendocrine cells in *Lymnaea stagnalis*. *J Neurochem*, 92(5), 1073-
739 1080. doi:10.1111/j.1471-4159.2004.02927.x
- 740 Ishizaki, H., Miyoshi, J., Kamiya, H., Togawa, A., Tanaka, M., Sasaki, T., . . . Takai, Y. (2000). Role of rab
741 GDP dissociation inhibitor alpha in regulating plasticity of hippocampal neurotransmission.
742 *Proc Natl Acad Sci U S A*, 97(21), 11587-11592. doi:10.1073/pnas.97.21.11587
- 743 Ito, E., Okada, R., Sakamoto, Y., Otshuka, E., Mita, K., Okuta, A., . . . Sakakibara, M. (2012). Insulin and
744 memory in *Lymnaea*. *Acta Biol Hung*, 63 Suppl 2, 194-201.
745 doi:10.1556/ABiol.63.2012.Suppl.2.25
- 746 Janse, C., Slob, W., Popelier, C. M., & Vogelaar, J. W. (1988). Survival characteristics of the mollusc
747 *Lymnaea stagnalis* under constant culture conditions: effects of aging and disease. *Mech*
748 *Ageing Dev*, 42(3), 263-274. doi:10.1016/0047-6374(88)90052-8
- 749 Jimenez, C. R., ter Maat, A., Pieneman, A., Burlingame, A. L., Smit, A. B., & Li, K. W. (2004). Spatio-
750 temporal dynamics of the egg-laying-inducing peptides during an egg-laying cycle: a
751 semiquantitative matrix-assisted laser desorption/ionization mass spectrometry approach. *J*
752 *Neurochem*, 89(4), 865-875. doi:10.1111/j.1471-4159.2004.02353.x
- 753 Ju, P., & Cui, D. (2016). The involvement of N-methyl-D-aspartate receptor (NMDAR) subunit NR1 in
754 the pathophysiology of schizophrenia. *Acta Biochim Biophys Sin (Shanghai)*, 48(3), 209-219.
755 doi:10.1093/abbs/gmv135
- 756 Kang, H. J., Kawasawa, Y. I., Cheng, F., Zhu, Y., Xu, X., Li, M., . . . Sestan, N. (2011). Spatio-temporal
757 transcriptome of the human brain. *Nature*, 478(7370), 483-489. doi:10.1038/nature10523
- 758 Kim, D., Langmead, B., & Salzberg, S. L. (2015). HISAT: a fast spliced aligner with low memory
759 requirements. *Nat Methods*, 12(4), 357-360. doi:10.1038/nmeth.3317
- 760 Kojima, S., Nanakamura, H., Nagayama, S., Fujito, Y., & Ito, E. (1997). Enhancement of an inhibitory
761 input to the feeding central pattern generator in *Lymnaea stagnalis* during conditioned taste-
762 aversion learning. *Neurosci Lett*, 230(3), 179-182. doi:10.1016/s0304-3940(97)00507-7
- 763 Kojima, S., Sunada, H., Mita, K., Sakakibara, M., Lukowiak, K., & Ito, E. (2015). Function of insulin in
764 snail brain in associative learning. *J Comp Physiol A Neuroethol Sens Neural Behav Physiol*,
765 201(10), 969-981. doi:10.1007/s00359-015-1032-5
- 766 Kuroda, R., & Abe, M. (2020). The pond snail *Lymnaea stagnalis*. *Evodevo*, 11(1), 24.
767 doi:10.1186/s13227-020-00169-4
- 768 Lambe, E. K., Fillman, S. G., Webster, M. J., & Shannon Weickert, C. (2011). Serotonin receptor
769 expression in human prefrontal cortex: balancing excitation and inhibition across postnatal
770 development. *PLoS One*, 6(7), e22799. doi:10.1371/journal.pone.0022799
- 771 Lansdell, S. J., Collins, T., Goodchild, J., & Millar, N. S. (2012). The *Drosophila* nicotinic acetylcholine
772 receptor subunits $\alpha 5$ and $\alpha 7$ form functional homomeric and heteromeric ion
773 channels. *BMC Neurosci*, 13, 73. doi:10.1186/1471-2202-13-73
- 774 Law, A. J., Weickert, C. S., Webster, M. J., Herman, M. M., Kleinman, J. E., & Harrison, P. J. (2003).
775 Expression of NMDA receptor NR1, NR2A and NR2B subunit mRNAs during development of
776 the human hippocampal formation. *Eur J Neurosci*, 18(5), 1197-1205. doi:10.1046/j.1460-
777 9568.2003.02850.x
- 778 Liao, Y., Smyth, G. K., & Shi, W. (2014). featureCounts: an efficient general purpose program for
779 assigning sequence reads to genomic features. *Bioinformatics*, 30(7), 923-930.
780 doi:10.1093/bioinformatics/btt656

- 781 Liu, M. M., Davey, J. W., Jackson, D. J., Blaxter, M. L., & Davison, A. (2014). A conserved set of
782 maternal genes? Insights from a molluscan transcriptome. *Int J Dev Biol*, *58*(6-8), 501-511.
783 doi:10.1387/ijdb.140121ad
- 784 Love, M. I., Huber, W., & Anders, S. (2014). Moderated estimation of fold change and dispersion for
785 RNA-seq data with DESeq2. *Genome Biol*, *15*(12), 550. doi:10.1186/s13059-014-0550-8
- 786 Lu, M. R., Lai, C. K., Liao, B. Y., & Tsai, I. J. (2020). Comparative Transcriptomics across Nematode Life
787 Cycles Reveal Gene Expression Conservation and Correlated Evolution in Adjacent
788 Developmental Stages. *Genome Biol Evol*, *12*(7), 1019-1030. doi:10.1093/gbe/evaa110
- 789 Maasz, G., Zrinyi, Z., Reglodi, D., Petrovics, D., Rivnyak, A., Kiss, T., . . . Pirger, Z. (2017). Pituitary
790 adenylate cyclase-activating polypeptide (PACAP) has a neuroprotective function in
791 dopamine-based neurodegeneration in rat and snail parkinsonian models. *Dis Model Mech*,
792 *10*(2), 127-139. doi:10.1242/dmm.027185
- 793 Mersman, B. A., Jolly, S. N., Lin, Z., & Xu, F. (2020). Gap Junction Coding Innexin in *Lymnaea stagnalis*:
794 Sequence Analysis and Characterization in Tissues and the Central Nervous System. *Front*
795 *Synaptic Neurosci*, *12*, 1. doi:10.3389/fnsyn.2020.00001
- 796 Mistry, J., Finn, R. D., Eddy, S. R., Bateman, A., & Punta, M. (2013). Challenges in homology search:
797 HMMER3 and convergent evolution of coiled-coil regions. *Nucleic Acids Res*, *41*(12), e121.
798 doi:10.1093/nar/gkt263
- 799 Montellano, O. d. (2015). *Cytochrome P450: structure, mechanism and biochemistry* (O. d.
800 Montellano Ed. 4th ed.): Kluwer Academic/Plenum Publishers.
- 801 Monyer, H., Burnashev, N., Laurie, D. J., Sakmann, B., & Seeburg, P. H. (1994). Developmental and
802 regional expression in the rat brain and functional properties of four NMDA receptors.
803 *Neuron*, *12*(3), 529-540. doi:10.1016/0896-6273(94)90210-0
- 804 Moroz, L. L., Edwards, J. R., Puthanveetil, S. V., Kohn, A. B., Ha, T., Heyland, A., . . . Kandel, E. R.
805 (2006). Neuronal transcriptome of *Aplysia*: neuronal compartments and circuitry. *Cell*,
806 *127*(7), 1453-1467. doi:10.1016/j.cell.2006.09.052
- 807 Moroz, L. L., & Kohn, A. B. (2010). Do different neurons age differently? Direct genome-wide analysis
808 of aging in single identified cholinergic neurons. *Front Aging Neurosci*, *2*.
809 doi:10.3389/neuro.24.006.2010
- 810 Moskalev, A. A., Shaposhnikov, M. V., Zemskaia, N. V., Koval Lcapital A, C., Schegoleva, E. V.,
811 Guvatova, Z. G., . . . Kudryavtseva, A. V. (2019). Transcriptome Analysis of Long-lived
812 *Drosophila melanogaster* E(z) Mutants Sheds Light on the Molecular Mechanisms of
813 Longevity. *Sci Rep*, *9*(1), 9151. doi:10.1038/s41598-019-45714-x
- 814 Murakami, J., Okada, R., Sadamoto, H., Kobayashi, S., Mita, K., Sakamoto, Y., . . . Ito, E. (2013).
815 Involvement of insulin-like peptide in long-term synaptic plasticity and long-term memory of
816 the pond snail *Lymnaea stagnalis*. *J Neurosci*, *33*(1), 371-383. doi:10.1523/JNEUROSCI.0679-
817 12.2013
- 818 Nance, M. A. (2017). Genetics of Huntington disease. *Handb Clin Neurol*, *144*, 3-14.
819 doi:10.1016/B978-0-12-801893-4.00001-8
- 820 Nikolac Perkovic, M., & Pivac, N. (2019). Genetic Markers of Alzheimer's Disease. *Adv Exp Med Biol*,
821 *1192*, 27-52. doi:10.1007/978-981-32-9721-0_3
- 822 Onizuka, S., Shiraishi, S., Tamura, R., Yonaha, T., Oda, N., Kawasaki, Y., . . . Tsuneyoshi, I. (2012).
823 Lidocaine treatment during synapse reformation periods permanently inhibits NGF-induced
824 excitation in an identified reconstructed synapse of *Lymnaea stagnalis*. *J Anesth*, *26*(1), 45-53.
825 doi:10.1007/s00540-011-1257-6
- 826 Ovsepiyan, S. V. (2017). The birth of the synapse. *Brain Struct Funct*, *222*(8), 3369-3374.
827 doi:10.1007/s00429-017-1459-2
- 828 Pacifico, R., MacMullen, C. M., Walkinshaw, E., Zhang, X., & Davis, R. L. (2018). Brain transcriptome
829 changes in the aging *Drosophila melanogaster* accompany olfactory memory performance
830 deficits. *PLoS One*, *13*(12), e0209405. doi:10.1371/journal.pone.0209405

- 831 Papke, R. L., Dwoskin, L. P., & Crooks, P. A. (2007). The pharmacological activity of nicotine and
832 nornicotine on nAChRs subtypes: relevance to nicotine dependence and drug discovery. *J*
833 *Neurochem*, *101*(1), 160-167. doi:10.1111/j.1471-4159.2006.04355.x
- 834 Pereda, A. E. (2014). Electrical synapses and their functional interactions with chemical synapses. *Nat*
835 *Rev Neurosci*, *15*(4), 250-263. doi:10.1038/nrn3708
- 836 Pertea, M., Pertea, G. M., Antonescu, C. M., Chang, T. C., Mendell, J. T., & Salzberg, S. L. (2015).
837 StringTie enables improved reconstruction of a transcriptome from RNA-seq reads. *Nat*
838 *Biotechnol*, *33*(3), 290-295. doi:10.1038/nbt.3122
- 839 Rackauskas, M., Neverauskas, V., & Skeberdis, V. A. (2010). Diversity and properties of connexin gap
840 junction channels. *Medicina (Kaunas)*, *46*(1), 1-12.
- 841 Sadamoto, H., Takahashi, H., Okada, T., Kenmoku, H., Toyota, M., & Asakawa, Y. (2012). De novo
842 sequencing and transcriptome analysis of the central nervous system of mollusc *Lymnaea*
843 *stagnalis* by deep RNA sequencing. *PLoS One*, *7*(8), e42546.
844 doi:10.1371/journal.pone.0042546
- 845 Seppala, O., Walser, J. C., Cereghetti, T., Seppala, K., Salo, T., & Adema, C. M. (2021). Transcriptome
846 profiling of *Lymnaea stagnalis* (Gastropoda) for ecoimmunological research. *BMC Genomics*,
847 *22*(1), 144. doi:10.1186/s12864-021-07428-1
- 848 Seshadri, S., Klaus, A., Winkowski, D. E., Kanold, P. O., & Plenz, D. (2018). Altered avalanche dynamics
849 in a developmental NMDAR hypofunction model of cognitive impairment. *Transl Psychiatry*,
850 *8*(1), 3. doi:10.1038/s41398-017-0060-z
- 851 Shavlakadze, T., Morris, M., Fang, J., Wang, S. X., Zhu, J., Zhou, W., . . . Glass, D. J. (2019). Age-Related
852 Gene Expression Signature in Rats Demonstrate Early, Late, and Linear Transcriptional
853 Changes from Multiple Tissues. *Cell Rep*, *28*(12), 3263-3273 e3263.
854 doi:10.1016/j.celrep.2019.08.043
- 855 Sodhi, M. S., & Sanders-Bush, E. (2004). Serotonin and brain development. *Int Rev Neurobiol*, *59*, 111-
856 174. doi:10.1016/S0074-7742(04)59006-2
- 857 Steen, W. J., Jager, J. H., & Hoven, N. P. V. D. (1968). A Method for Breeding and Studying Freshwater
858 Snails Under Continuous Water Change, With Some Remarks On Growth and Reproduction in
859 *Lymnaea Stagnalis* (L.). *Netherlands Journal of Zoology*, *19*, 131-139.
- 860 Sunada, H., Watanabe, T., Hatakeyama, D., Lee, S., Forest, J., Sakakibara, M., . . . Lukowiak, K. (2017).
861 Pharmacological effects of cannabinoids on learning and memory in *Lymnaea*. *J Exp Biol*,
862 *220*(Pt 17), 3026-3038. doi:10.1242/jeb.159038
- 863 Swinton, C., Swinton, E., Shymansky, T., Hughes, E., Zhang, J., Rothwell, C., . . . Lukowiak, K. (2019).
864 Configural learning: a higher form of learning in *Lymnaea*. *J Exp Biol*, *222*(Pt 3).
865 doi:10.1242/jeb.190405
- 866 Syed, N. I., & Winlow, W. (1991). Coordination of locomotor and cardiorespiratory networks of
867 *Lymnaea stagnalis* by a pair of identified interneurons. *J Exp Biol*, *158*, 37-62.
- 868 Tan, R., & Lukowiak, K. (2018). Combining Factors That Individually Enhance Memory in *Lymnaea*.
869 *Biol Bull*, *234*(1), 37-44. doi:10.1086/697197
- 870 Tarkhov, A. E., Alla, R., Ayyadevara, S., Pyatnitskiy, M., Menshikov, L. I., Shmookler Reis, R. J., &
871 Fedichev, P. O. (2019). A universal transcriptomic signature of age reveals the temporal
872 scaling of *Caenorhabditis elegans* aging trajectories. *Sci Rep*, *9*(1), 7368. doi:10.1038/s41598-
873 019-43075-z
- 874 Taylor, B. E., & Lukowiak, K. (2000). The respiratory central pattern generator of *Lymnaea*: a model,
875 measured and malleable. *Respir Physiol*, *122*(2-3), 197-207. doi:10.1016/s0034-
876 5687(00)00159-6
- 877 Team, R. C. (2017). R: A language and environment for statistical computing. Vienna, Austria: R
878 Foundation for Statistical Computing. Retrieved from <https://www.r-project.org/>
- 879 Tebbenkamp, A. T., Willsey, A. J., State, M. W., & Sestan, N. (2014). The developmental
880 transcriptome of the human brain: implications for neurodevelopmental disorders. *Curr Opin*
881 *Neurol*, *27*(2), 149-156. doi:10.1097/WCO.0000000000000069

- 882 Teranishi, Y., Inoue, M., Yamamoto, N. G., Kihara, T., Wiehager, B., Ishikawa, T., . . . Tjernberg, L. O.
883 (2015). Proton myo-inositol cotransporter is a novel gamma-secretase associated protein
884 that regulates Abeta production without affecting Notch cleavage. *FEBS J*, 282(17), 3438-
885 3451. doi:10.1111/febs.13353
- 886 Teunissen, Y., Geraerts, W. P., van Heerikhuizen, H., Planta, R. J., & Joosse, J. (1992). Molecular
887 cloning of a cDNA encoding a member of a novel cytochrome P450 family in the mollusc
888 *Lymnaea stagnalis*. *J Biochem*, 112(2), 249-252. doi:10.1093/oxfordjournals.jbchem.a123885
- 889 van Nierop, P., Bertrand, S., Munno, D. W., Gouwenberg, Y., van Minnen, J., Spafford, J. D., . . . Smit,
890 A. B. (2006). Identification and functional expression of a family of nicotinic acetylcholine
891 receptor subunits in the central nervous system of the mollusc *Lymnaea stagnalis*. *J Biol*
892 *Chem*, 281(3), 1680-1691. doi:10.1074/jbc.M508571200
- 893 van Nierop, P., Keramidas, A., Bertrand, S., van Minnen, J., Gouwenberg, Y., Bertrand, D., & Smit, A.
894 B. (2005). Identification of molluscan nicotinic acetylcholine receptor (nAChR) subunits
895 involved in formation of cation- and anion-selective nAChRs. *J Neurosci*, 25(46), 10617-
896 10626. doi:10.1523/JNEUROSCI.2015-05.2005
- 897 Vesterlund, L., Jiao, H., Unneberg, P., Hovatta, O., & Kere, J. (2011). The zebrafish transcriptome
898 during early development. *BMC Dev Biol*, 11, 30. doi:10.1186/1471-213X-11-30
- 899 Vorontsov, D. D., Tsyganov, V. V., & Sakharov, D. A. (2004). Phasic coordination between locomotor
900 and respiratory rhythms in *Lymnaea*. Real behavior and computer simulation. *Acta Biol Hung*,
901 55(1-4), 233-237. doi:10.1556/ABiol.55.2004.1-4.28
- 902 Wang, B., Wangkahart, E., Secombes, C. J., & Wang, T. (2019). Insights into the Evolution of the
903 Suppressors of Cytokine Signaling (SOCS) Gene Family in Vertebrates. *Mol Biol Evol*, 36(2),
904 393-411. doi:10.1093/molbev/msy230
- 905 Xia, X., Ding, M., Xuan, J. F., Xing, J. X., Pang, H., Wang, B. J., & Yao, J. (2018). Polymorphisms in the
906 human serotonin receptor 1B (HTR1B) gene are associated with schizophrenia: a case control
907 study. *BMC Psychiatry*, 18(1), 303. doi:10.1186/s12888-018-1849-x
- 908 Xu, Z., Che, T., Li, F., Tian, K., Zhu, Q., Mishra, S. K., . . . Li, D. (2018). The temporal expression patterns
909 of brain transcriptome during chicken development and ageing. *BMC Genomics*, 19(1), 917.
910 doi:10.1186/s12864-018-5301-x
- 911 Yang, Y. S., & Strittmatter, S. M. (2007). The reticulons: a family of proteins with diverse functions.
912 *Genome Biol*, 8(12), 234. doi:10.1186/gb-2007-8-12-234
- 913 Yeoman, M. S., Kemenes, G., Benjamin, P. R., & Elliott, C. J. (1994). Modulatory role for the
914 serotonergic cerebral giant cells in the feeding system of the snail, *Lymnaea*. II.
915 Photoinactivation. *J Neurophysiol*, 72(3), 1372-1382. doi:10.1152/jn.1994.72.3.1372
- 916 Zhang, X., Liu, C., Miao, H., Gong, Z. H., & Nordberg, A. (1998). Postnatal changes of nicotinic
917 acetylcholine receptor alpha 2, alpha 3, alpha 4, alpha 7 and beta 2 subunits genes
918 expression in rat brain. *Int J Dev Neurosci*, 16(6), 507-518. doi:10.1016/s0736-
919 5748(98)00044-6
- 920 Zhang, Y., Zhao, J., Zhang, H., Gai, Y., Wang, L., Li, F., . . . Song, L. (2010). The involvement of
921 suppressors of cytokine signaling 2 (SOCS2) in immune defense responses of Chinese mitten
922 crab *Eriocheir sinensis*. *Dev Comp Immunol*, 34(1), 42-48. doi:10.1016/j.dci.2009.08.001
- 923 Zoli, M., Pistillo, F., & Gotti, C. (2015). Diversity of native nicotinic receptor subtypes in mammalian
924 brain. *Neuropharmacology*, 96(Pt B), 302-311. doi:10.1016/j.neuropharm.2014.11.003

925

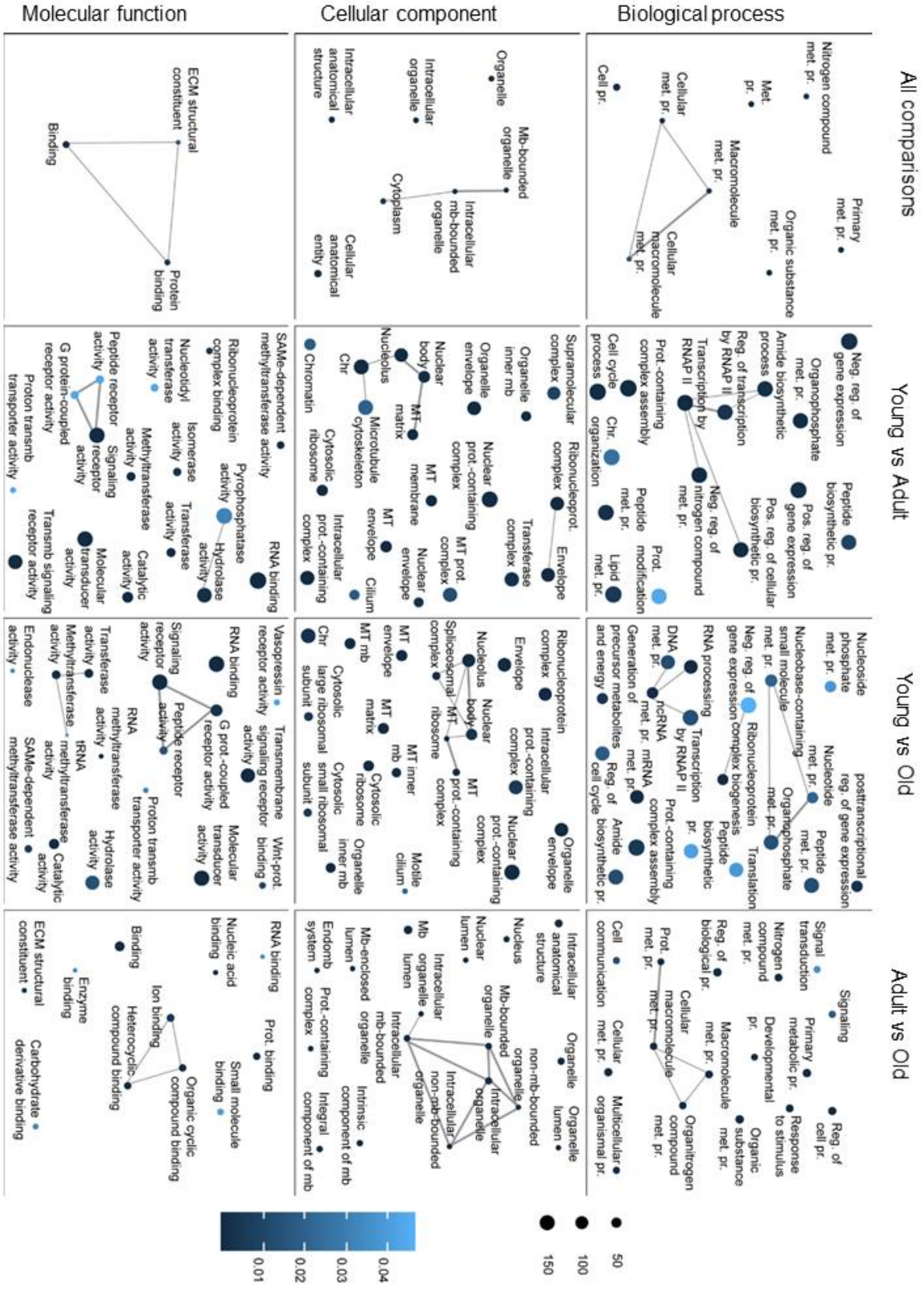


926

927 **Figure 1. Pairwise comparisons of transcriptomes reveal a specific pattern of gene**
 928 **expression in the CNS of young *L. stagnalis*.** A) For transcriptome analysis, mRNA was
 929 extracted from the CNS of young (3 months old), adult (6 months old), and old (18 months
 930 old) snails. For each age group, four different biological replicates ($n = 4$), each with mRNA
 931 samples from the CNS of 10 snails, were used. B) Venn diagram showing the significantly
 932 differentially expressed genes in each pairwise comparison and the overlap among them.
 933 The diagram clearly shows that young CNS transcriptome has more significantly differentially
 934 expressed genes compared to adult and old. (FDR adjusted p -value $p < 0.05$; log2 fold
 935 change $> |1|$). C) Volcano plot of each pairwise comparison. The plots are color-coded based
 936 on the log2 fold change (green dots), and corrected p -value (blue dots). Red dots highlight
 937 genes that are significant and whose expression is highly changed (FDR adjusted p -value p
 938 < 0.05 ; log2 fold change $> |1|$). Volcano plots of the comparison between adult and old CNS
 939 transcriptome shows less differentially expressed genes, by either p -value or log2 fold-
 940 change, compared to the pairwise comparison of young versus adult or old transcriptome. D,
 941 E) Heatmap of the most differentially expressed genes in all pairwise comparisons (FDR
 942 adjusted p -value $p < 0.05$) and the genes with the highest variance (top 2000 genes),
 943 respectively. Both heatmaps show a distinct pattern of gene expression in the CNS
 944 transcriptome of young snails compared to adult and old.

945

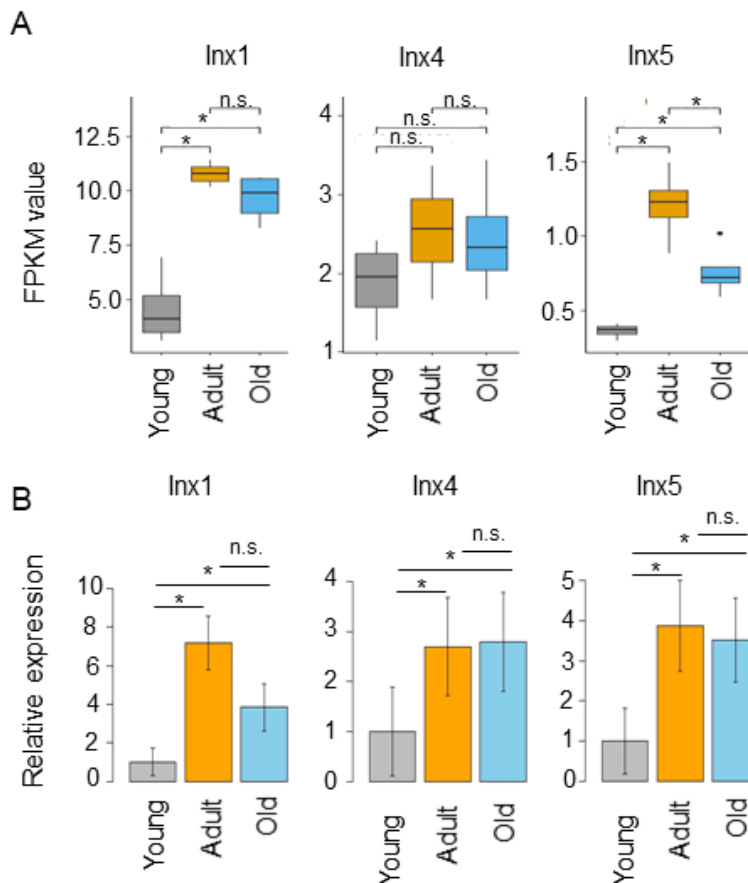
946



947

948 **Figure 2. Gene Ontology (GO) enrichment analysis of differentially expressed genes.**
 949 Representative enriched GO terms are shown as dots for each GO category (Biological
 950 process, Cellular component, or Molecular function). The significantly differentially expressed
 951 genes in all pairwise comparisons (All comparisons, 455 genes), in the comparison between
 952 young and adult CNS transcriptomes (Young vs. Adult, 20,141 genes), young and old CNS
 953 transcriptomes (Young vs. Old, 18,394 genes), or adult and old CNS transcriptomes (Adult
 954 vs Old, 3,108 genes) were used for the analysis. The dot size reflects the number of genes in
 955 the GO term for each significantly differentially expressed gene set; the dot colour represents
 956 the FDR-corrected p -value, with darker colours indicating lower p -values; the line size
 957 represents the degree of similarity. Abbreviations: met. = metabolic, pr. = process, neg. =
 958 negative, pos. = positive, reg. = regulation, mb = membrane, prot. = protein, chr =
 959 chromosome, RNAP II = RNA polymerase II, MT = mitochondrial, ECM = extracellular matrix.

960
 961
 962

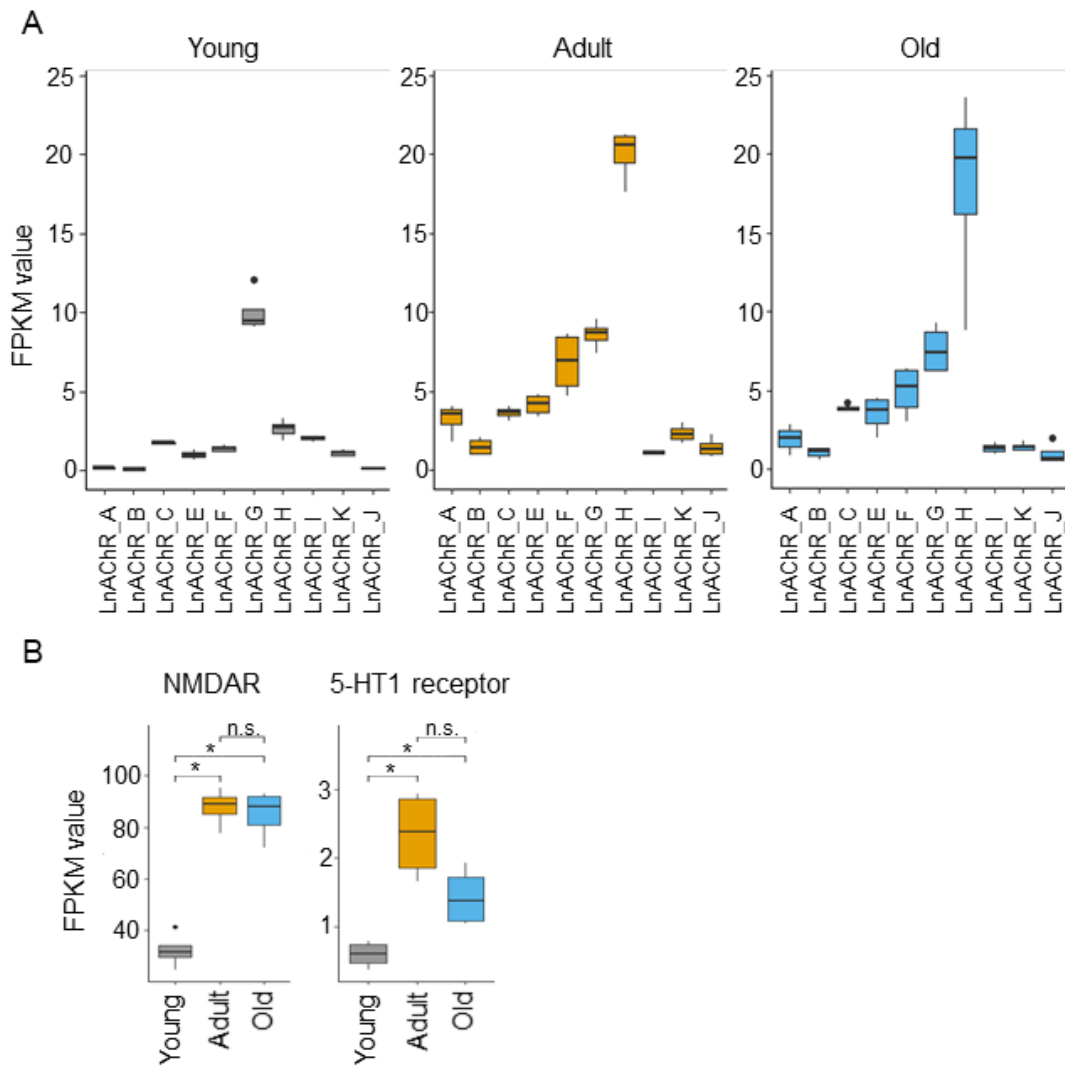


963
 964 **Figure 3. Confirmation of differential gene expression by real-time qPCR of *L. stagnalis* Innexin genes.** A) RNA-Seq data reveals lower gene expression for innexins in
 965 young snails CNS compared to adult and old. B) real-time qPCR data show patterns of
 966 expression comparable to RNA-Seq data. These data show a general concordance of gene
 967 expression measured in our transcriptome data compared to qPCR data. * $p < 0.05$.

969
 970

971

972



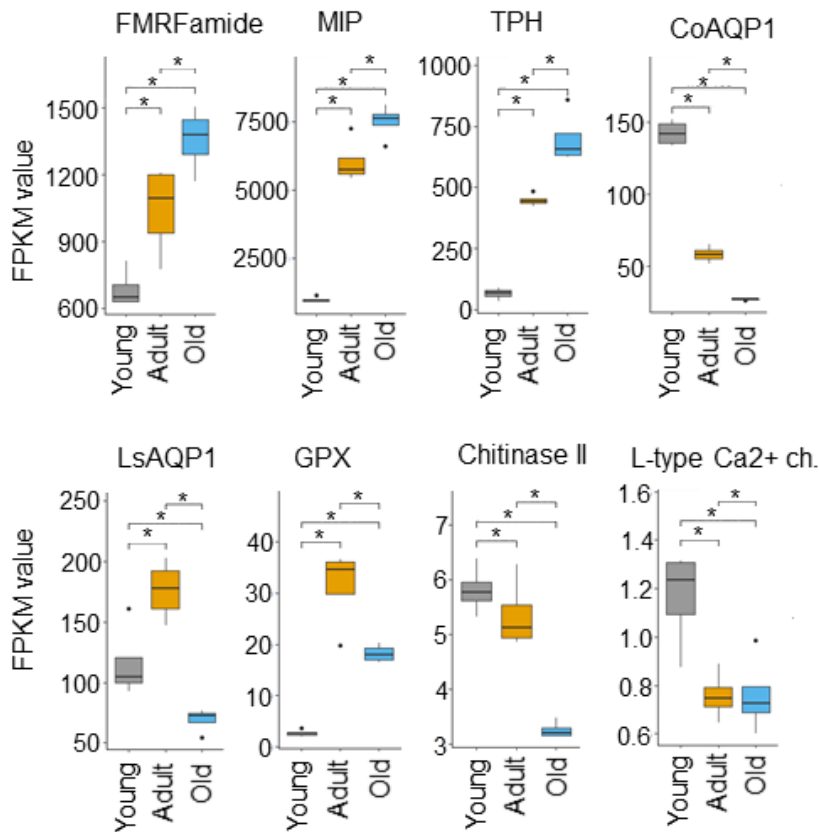
973

974 **Figure 4. Differential expression of previously cloned synaptic receptor genes in *L.***
 975 ***stagnalis*.** A) FPKM expression of different *L. stagnalis* acetylcholine receptor subunits
 976 (LnAChR). Consistent with previous literature, the most highly expressed subunit in adult
 977 CNS transcriptome is the subunit H. Old snail CNS transcriptome has a similar pattern of
 978 LnAChR expression as adult snails. In young snails, though, the most highly expressed
 979 subunit is G. These data suggest that acetylcholine receptor subunits are specifically
 980 expressed at different life stages. B) Genes involved in synaptic transmission (NMDAR, N-
 981 Methyl-D-aspartic acid receptor; 5-HT receptor, and serotonin receptor) are significantly
 982 downregulated in young snails CNS compared to adult and old. The different patterns of
 983 expression for neurotransmitter receptors in young versus adult and old snails suggest that
 984 CNS synaptic development requires specific patterning to establish functional synapses
 985 throughout the span of *L. stagnalis* life. * $p < 0.05$.

986

987

988



989

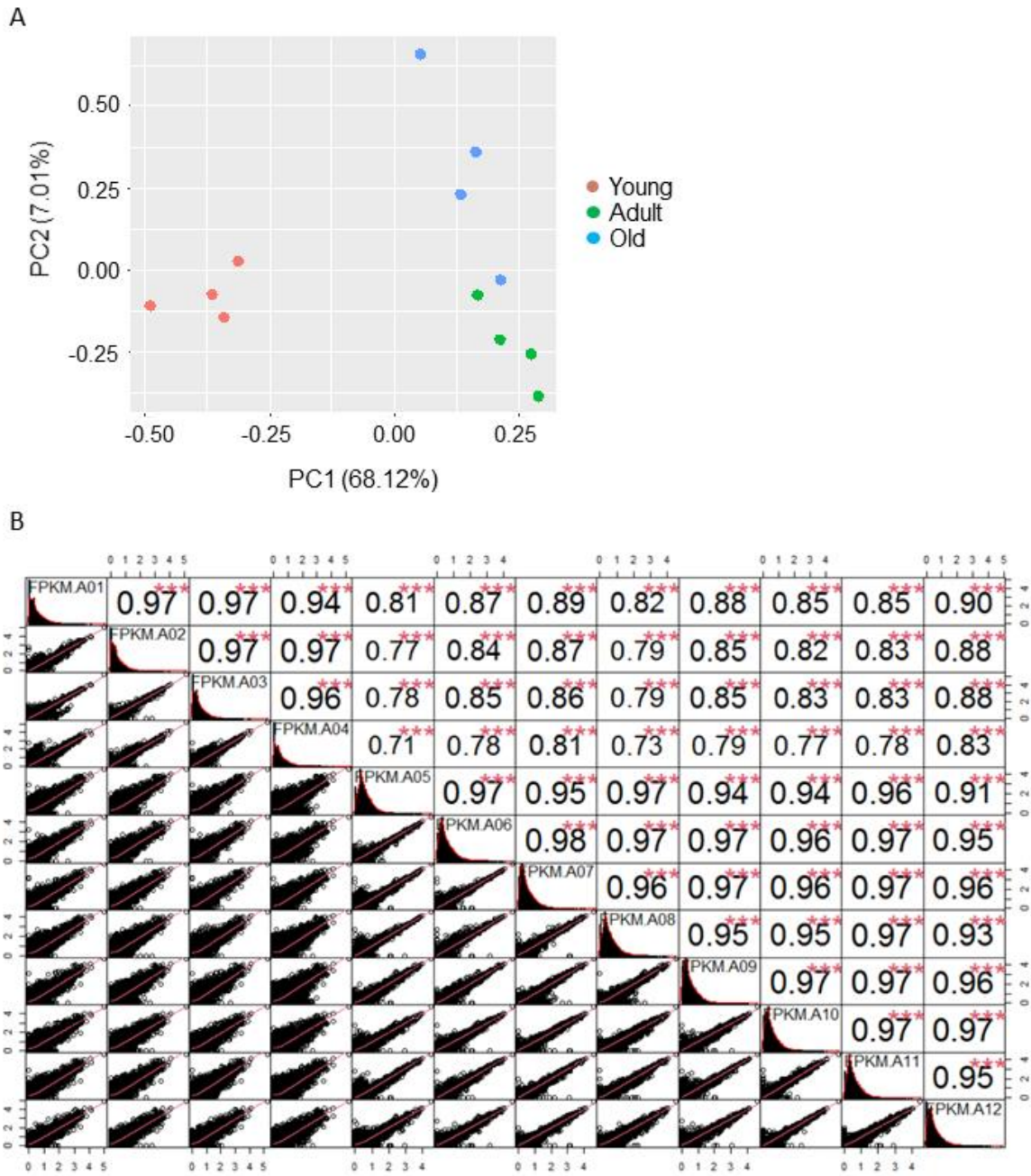
990 **Figure 5. Cloned genes with significantly different expression at all pairwise**
991 **comparisons.** The figure shows eight of the nine genes (*Inx5* is shown in Figure 3A), among
992 known cloned genes, that show significant changes in expression in all pairwise comparisons
993 (young vs adult, young vs old, adult vs old) (FDR adjusted p -value $p < 0.05$). Differential
994 expression of known genes suggests regulation of related pathways (e.g. long-term memory
995 formation for MIP) in the *L. stagnalis* central nervous system at different ages. MIP,
996 molluscan insulin peptide; TPH, tryptophane hydroxylase; AQP1, aquaporin1; GPX,
997 glutathione peroxidase. * $p < 0.05$.

998

999

1000

1001

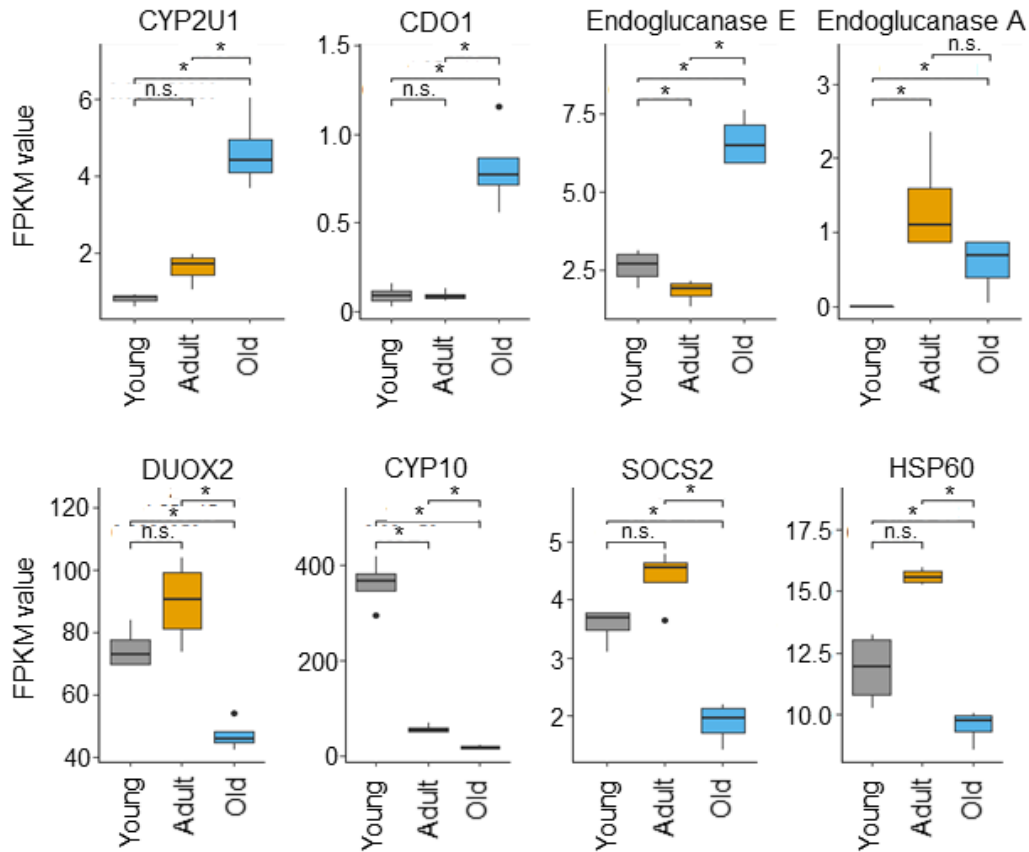


1002

1003 **Supplemental Figure 1. Data exploration of CNS transcriptomes reveal age-dependent**
 1004 **separation of samples.** A) Principal component analysis (PCA) shows a clear separation of
 1005 different developmental age samples. The first component (x-axis) explains ~68% of sample
 1006 separation and clearly separates the CNS transcriptome of young snails from adult and old.
 1007 The second component (y-axis) separates adult and old samples. B) Correlation analysis of
 1008 gene expression profile shows high correlations among samples that belong to the same
 1009 group (young snails CNS transcriptome, samples A01-A04; adult snails CNS transcriptome,
 1010 samples A05-A08; old snails CNS transcriptome, samples A09-A12)

1011

1012



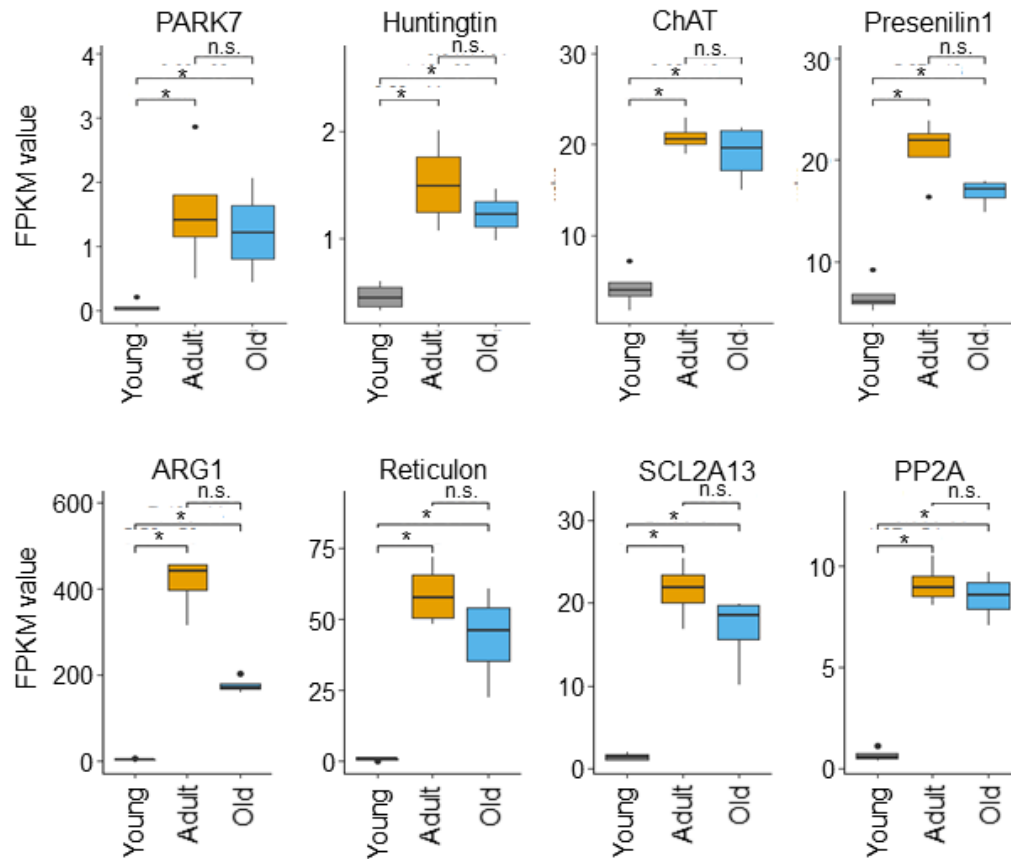
1013

1014 **Supplemental Figure 2. Differential expression of stress-related genes.** Selected DE
1015 genes involved in stress and immune response demonstrate differential expression patterns.
1016 Cytochrome P450 (CYP2U1), cysteine dioxygenase type 1 (CDO1), Endoglucanase E,
1017 Endoglucanase A, dual oxidase 2 (DUOX2), cytochrome P450 (CYP10), suppressor of
1018 cytokine signaling 2 (SOCS2), and heat shock protein 60 (HSP60).

1019

1020

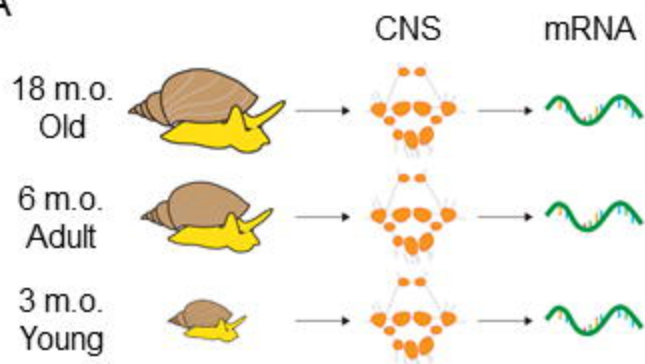
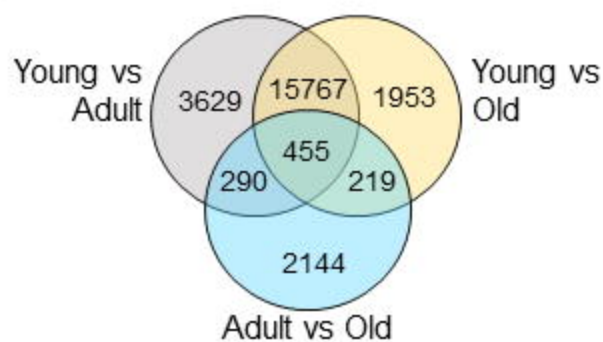
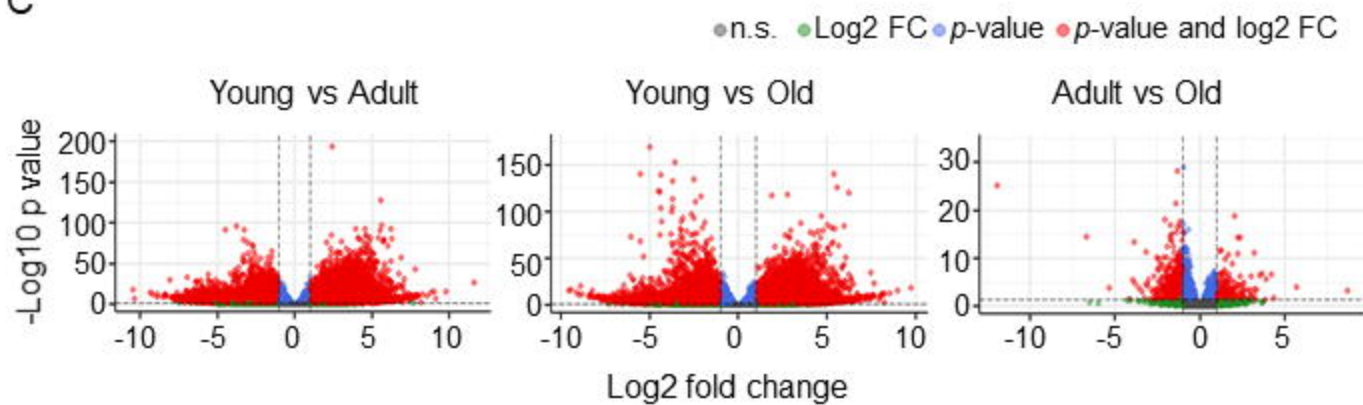
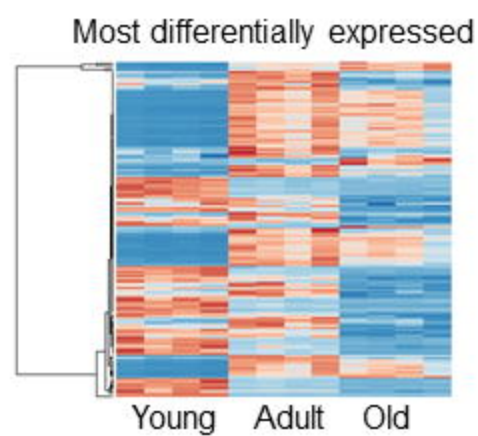
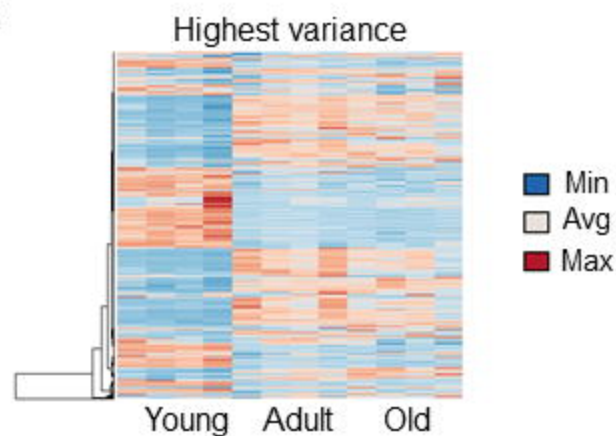
1021



1022

1023 **Supplemental Figure 3. Differential expression of disease-related genes.** Disease
1024 related genes have lowest levels of expression in young snails. Parkinson's disease protein 7
1025 (PARK7), huntingtin, choline acetyltransferase (ChAT), presenilin 1, arginase-1 (ARG-1),
1026 reticulon, membrane proton myo-inositol cotransporter (SCL2A13), and protein phosphatase
1027 2A (PP2A).

1028

A**B****C****D****E**

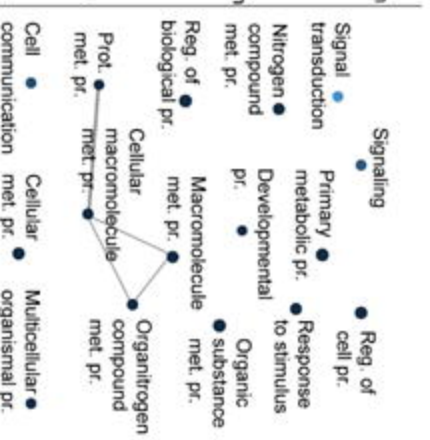
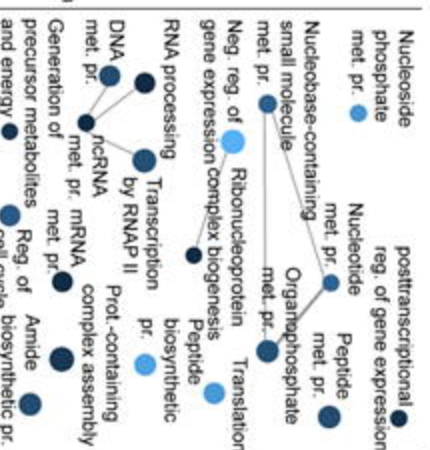
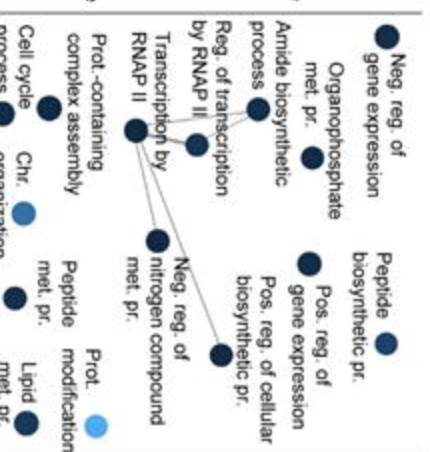
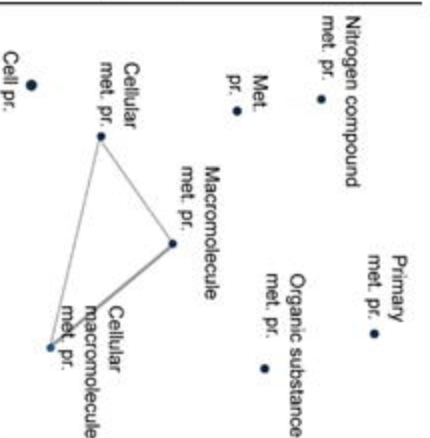
All comparisons

Young vs Adult

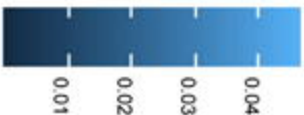
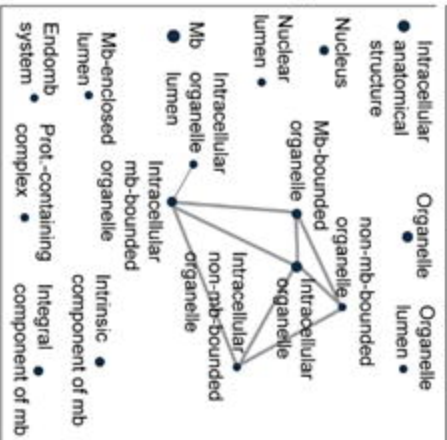
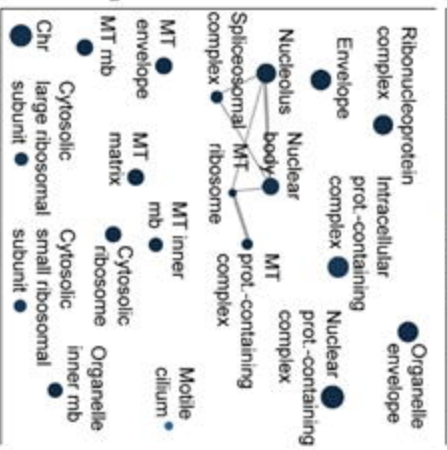
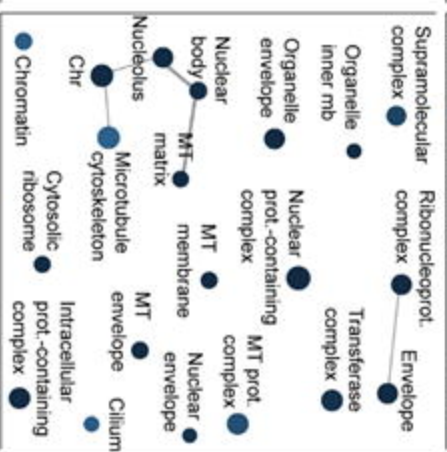
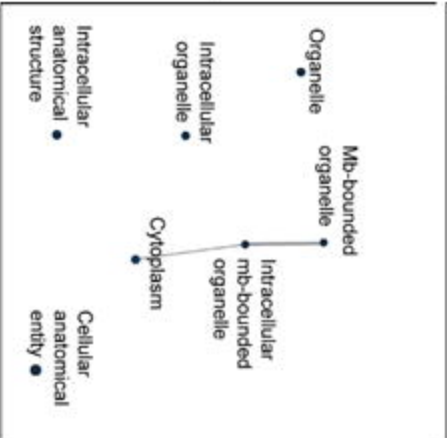
Young vs Old

Adult vs Old

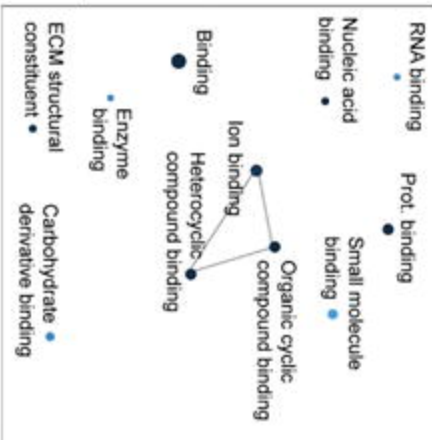
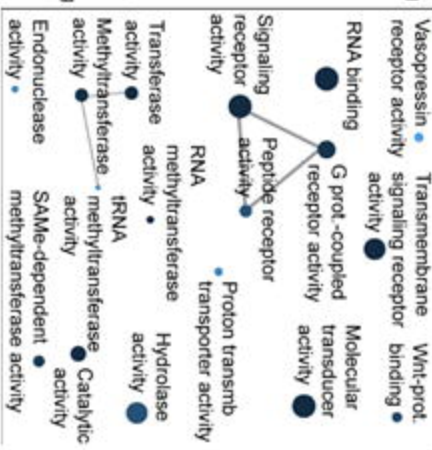
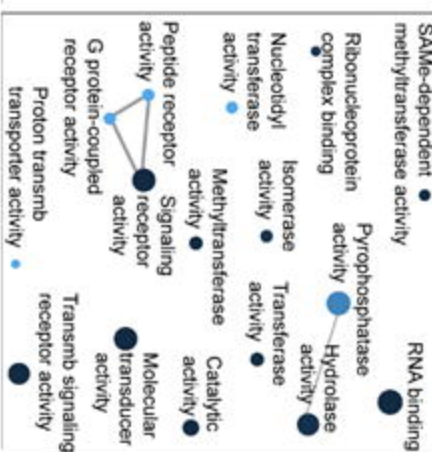
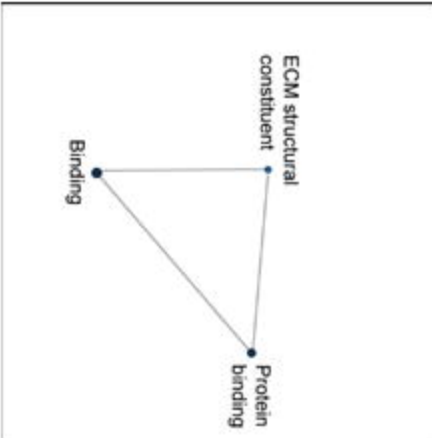
Biological process

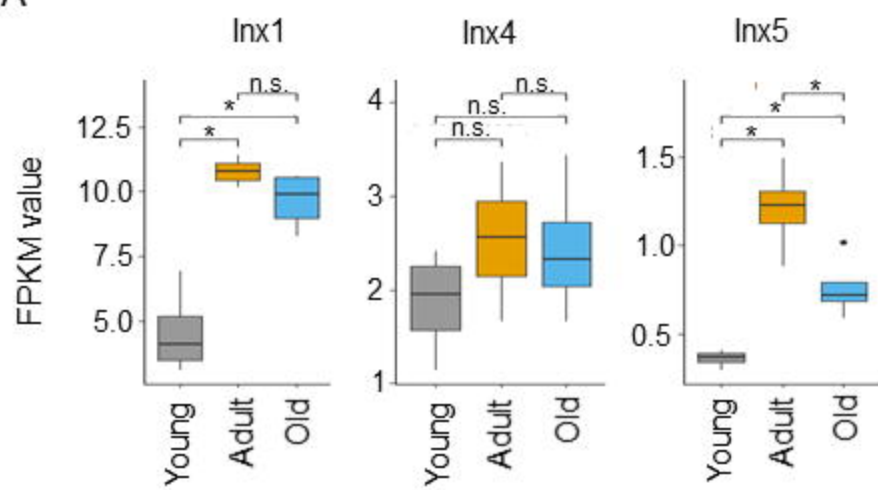
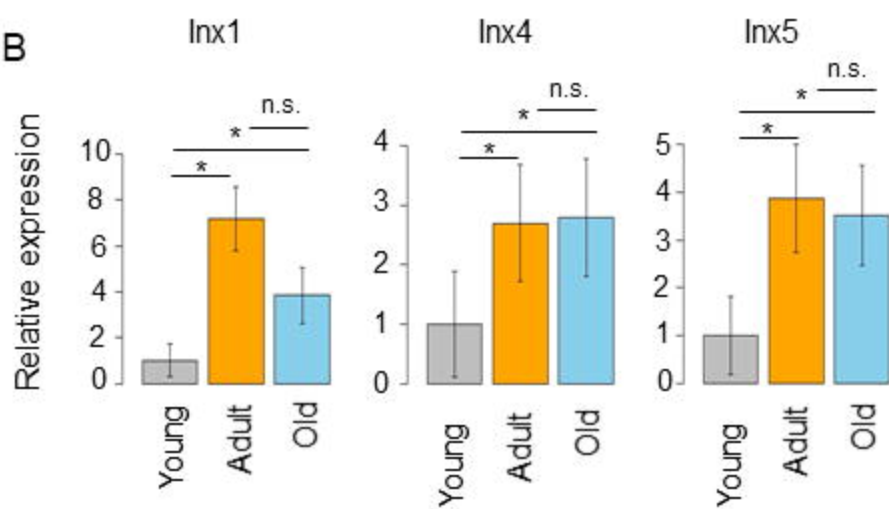


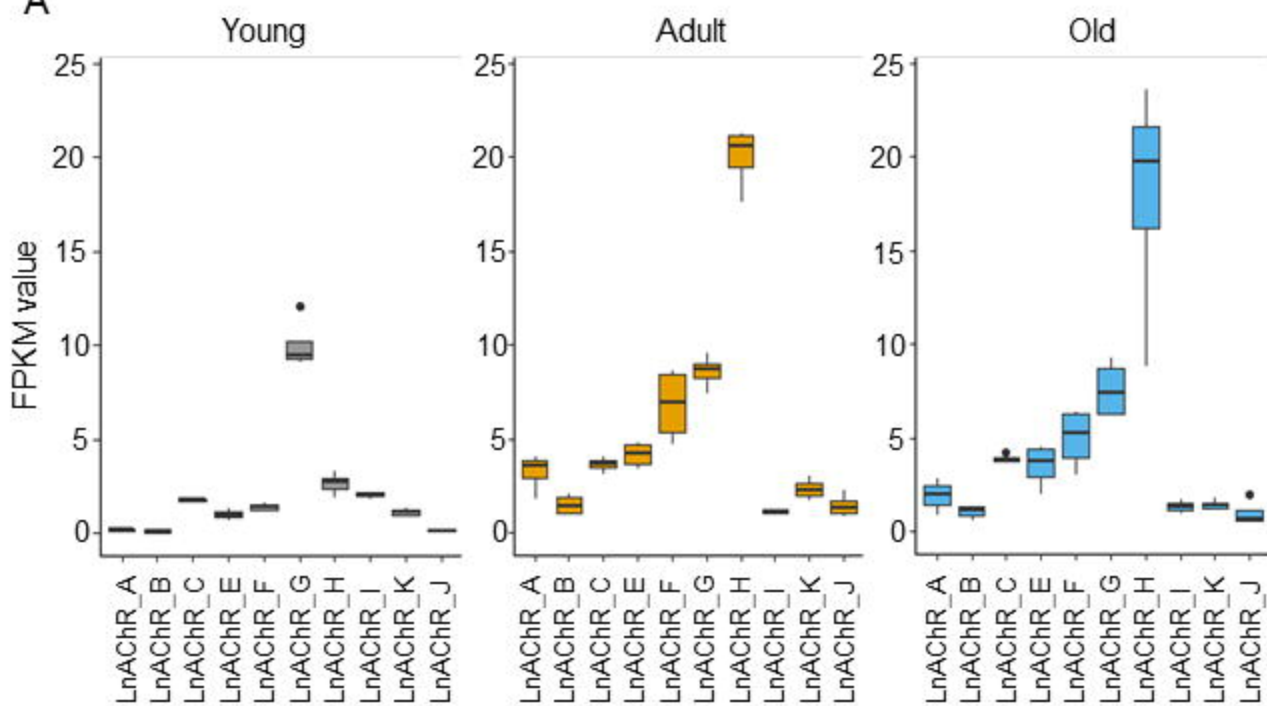
Cellular component



Molecular function



A**B**

A**B**